THEORETICAL CHEMISTRY INSTITUTE

100p

THE UNIVERSITY OF WISCONSIN

QUANTUM EFFECTS IN ELASTIC MOLECULAR SCATTERING

by

Richard B. Bernstein

WIS-TCI-47 1 June 1964

MADISON, WISCONSIN

QUANTUM EFFECTS IN ELASTIC MOLECULAR SCATTERING*

by

Richard B. Bernstein

Theoretical Chemistry Institute and Chemistry Department

University of Wisconsin, Madison, Wisconsin

1 June 1964

This manuscript is to be published by John Wiley and Sons in a volume entitled "Molecular Beams", edited by J. Ross, part of the Advances in Chemical Physics series, I. Prigogine, editor.

- - - - -

* This research received financial support from the U. S. Atomic Energy Commission, Division of Research and the National Aeronautics and Space Administration, Grant NsG-275-62(4180).

DDC
RECEIVED
JUN 29 1964
DDC-IRA A

QUANTUM EFFECTS IN ELASTIC MOLECULAR SCATTERING

TABLE OF CONTENTS

		page
I.	Introduction	1
II.	Resumé of Classical Treatment of Potential Scattering	3
III.	Resumé of Quantum Scattering Treatment	9
IV.	Approximation Methods	14
	a. The radial wave function	15
	b. The phase shifts	18
V.	The Scattering Amplitude	22
VI.	The Interference Pattern	28
VII.	Rainbow Scattering	33
VIII.	Low-Angle Scattering	37
IX.	Glory Interference Effect at Low Angles	47
X.	Total Elastic Cross Section	51
XI.	Extrema in Total Cross Sections	56
XII.	Maxima in Impact Spectra and the Bound States	61
XIII.	Influence of Concurrent Inelastic Processes	64
XIV.	References	74
XV.	Figures	80

QUANTUM EFFECTS IN ELASTIC MOLECULAR SCATTERING

I. Introduction

Observations of elastic scattering of atoms and molecules may be accounted for, to a large extent, by classical mechanics alone. However, a number of important features of the scattering behavior require a quantum mechanical interpretation; it is these which comprise the subject matter of this chapter.

Preparatory to a detailed discussion we shall outline the main points of difference between the classical and quantum results. We will compare the classical with the quantum predictions in each case; anticipating somewhat the final conclusions, it is found quite generally that experiment accords with the latter.

First we consider the differential cross sections, designated $I(\theta)$ $\left[\text{or } \frac{d\sigma(\theta)}{d\Omega}\right]$, for elastic scattering by a realistic intermolecular potential. The purely classical description yields a well-known unphysical singularity in the forward scattering, while the quantum treatment predicts a finite I(0). The classical inverse-power divergence in the low-angle scattering, $I(\theta) \propto \theta^{-7/3}$, is replaced by a well-behaved small-angle dependence, $I(\theta) \propto e^{-c\theta^2}$, according to the quantum treatment. The classical smooth dependence of differential cross section upon scattering angle is to be contrasted with the strongly oscillatory deBroglie interference pattern in $I(\theta)$ predicted by quantum theory.

With regard to the total elastic cross section, designated $Q(v_r)$ or $\sigma(v_r)$, the classical low angle divergence noted above

leads to an infinite value, while the quantum theory correctly yields a finite Q. The simplest quantum mechanical treatment, considering only the long-range r^{-6} attractive part of the interaction, accounts for the main part of the dependence of the cross section upon relative velocity, $Q \propto v_r^{-2/5}$. A more complete quantum analysis taking cognizance of the attractive potential well, predicts extrema (resonant behavior) in $Q(v_r)$ and suggests their relation to the bound states of the composite system. None of these features are encompassed within the classical framework.

In the discussion which follows, the emphasis will be upon the deviations from classical behavior predicted by the quantum mechanical and semiclassical treatments.*

- - - - -

* Most of the quantum effects with which we shall be concerned may be treated advantageously using the so-called "semiclassical approximation", valid when the deBroglie wavelength of the colliding system is comparable to or less than the "range" of the intermolecular forces. For very low energy collisions where this condition no longer obtains a full quantum mechanical treatment is required.

- - - - -

II. Resumé of Classical Treatment[1] of Potential Scattering

We assume an orientation-averaged, spherically symmetrical potential $V(r)$ with a long-range attraction, an attractive well and short-range repulsion[*].

- - - - -

[*] It is often convenient to write $V(r)$ in dimensionless form $V(r) = \epsilon V^*(x)$; here ϵ is the depth of the attractive well; $x = r/\sigma$, where σ is a characteristic length, here the zero of the potential (an alternative choice for a characteristic length is r_m, the position of the minimum in $V(r)$). Any potential with a minimum must contain at least two parameters; thus the function V^* often includes a number of constants governing the shape of the potential. Commonly used forms of the potential describing the interaction of ground state atoms and molecules include the Lennard-Jones (n,6), the Exp (α, 6), the Morse (β), the Kihara (α, 12, 6) and others, discussed in standard works[1a]. The simplest potential capable of accounting for the gross observed features of molecular scattering is the L.-J. (12,6) function, for which $V^*(x) = 4(x^{-12} - x^{-6})$. For the purpose of numerical or graphical illustration of some of the subsequent relationships between the potential, the angular deflection function and the scattering cross sections, we shall often employ the L.-J. (12,6) function. Of course, the main body of the formalism itself is quite general and may be applied to any well-behaved, realistic central potential.

- - - - -

From elementary considerations of energy and momentum conservation one obtains[1] an explicit expression for the classical deflection function, Θ (or χ).

$$\Theta(b, E) = \pi - 2b\int_{r_0}^{\infty} dr/r^2 F_c(r) \tag{II.1}$$

where $$F_c(r) = \left[1 - V(r)/E - b^2/r^2\right]^{1/2} ; \tag{II.2}$$

here b is the impact parameter, E the initial relative kinetic energy or "collision energy" ($E = \frac{1}{2}\mu v_r^2$, where μ is the reduced mass and v_r the magnitude of the relative velocity) and r_0 is the distance of closest approach in the encounter, or the "classical turning point" of the motion, seen to be the outermost zero of $F_c(r)$. It is recalled that the deflection function[2] Θ is positive for net repulsive and negative for net attractive trajectories; the observable scattering angle is $\theta = |\Theta|$ with $0 \leq \theta \leq \pi$.

In Fig. 1 is shown a typical curve of the dependence of the deflection function upon the reduced impact parameter $\beta \equiv b/\sigma$ for a definite value of the reduced collision energy $K \equiv E/\epsilon = 1.6$. The positive branch is associated with domination of repulsion, the negative branch with predominance of the attractive forces.

The differential solid-angle scattering cross section is expressible[1-3] directly in terms of the deflection function by

$$\frac{d\sigma(\theta)}{d\Omega} = \sum_{i=1}^{3} b_i \Big/ \sin\theta \cdot \left| \frac{d\Theta}{db_i} \right| \qquad \text{(II.3)}$$

where the summation is over the three possible regions of the deflection function contributing to the scattering at an angle θ . The forward scattering singularity previously mentioned is immediately evident from Eq. 3. A less obvious classical singularity, pointed out by Mason[3], occurs at $\theta = \theta_r$ (where $\frac{d\Theta}{db} = 0$); it has been termed[2] the "rainbow effect". It is seen that for $\theta > \theta_r$ only one region of the deflection function contributes to the scattering, while three regions do so for $\theta < \theta_r$. Thus there is a discontinuity as well as a singularity in the classical differential cross section at the rainbow angle (this angle corresponds to the trajectory of maximum attraction between the interacting particles).

In certain applications it is convenient to deal with a "reduced" differential cross section, i.e., $\frac{d\sigma(\theta)}{d\Omega}$ expressed in units of $\pi\sigma^2$ sometimes designated $I^*(\theta)$. Eq. 3 may be re-written, introducing other dimensionless parameters, as follows

$$I^*(\theta) \equiv \frac{d\sigma(\theta)}{d\Omega} \Big/ \pi\sigma^2 = \sum_{i=1}^{3} \left| \frac{dB_i}{dC} \right| \qquad \text{(II.4)}$$

where $C \equiv \cos\theta$, $B = \beta^2/2\pi$, and $\beta \equiv b/\sigma$ (the reduced impact parameter).

A suitable graphical presentation of Eq. 4 is shown in Fig. 2 (obtained directly from the deflection function of Fig. 1); it may be designated a BC plot. At any value of θ (or C), the classical

reduced differential cross section $I^*(\theta)$ is given by the sum of the absolute values of the slopes of the contributing branches of the BC plot. The forward singularity (C = 1) as well as the rainbow singularity and discontinuity are immediately obvious.

Fig. 3 shows a polar plot of $I^*(\theta)$ corresponding to the example of Fig. 2. Suggested but not shown is the strong forward divergence; the rainbow effect is clearly seen.

Returning to the deflection function, given by Eq. 1, it is well known[1] that except for trivial potential functions numerical integration is required to evaluate $\Theta(b, E)$ and thus $\frac{d\sigma(\theta)}{d\Omega}$ in the general case. However, for small angles one may employ the Kennard[1b] approximation for the deflection function. For large b (and thus small θ), where $r_0 \cong b$ and $V(r_0)/E \ll 1$, F(r) may be suitably expanded and the integration for Θ readily accomplished. For a potential with a long-range attraction of the form $V = -C^{(s)} r^{-s}$ one obtains*

$$\Theta \cong -(s-1) f(s)\, C^{(s)}/E b^{s} \tag{II.5}$$

and

$$\frac{d\sigma(\theta)}{d\Omega} \cong \left[(s-1) f(s)\right]^{2/s} \cdot s^{-1} \cdot \left[\frac{C^{(s)}}{E}\right]^{\frac{2}{s}} \Big/ \theta^{1+\frac{2}{s}} \cdot \sin\theta \cong g(s) \left[\frac{C^{(s)}}{E}\right]^{2/s} \cdot \theta^{-2(1+1/s)} \tag{II.6}$$

where $f(s) = \frac{1}{2}\pi^{1/2}\,\Gamma(\frac{1}{2}s - \frac{1}{2})/\Gamma(\frac{1}{2}s)$ and $g(s) = \left[(s-1) f(s)\right]^{2/s} \cdot s^{-1}$

- - - - -

* For the important practical case of s = 6, $f(6) = 3\pi/16$ and

$$\frac{d\sigma(\theta)}{d\Omega} \cong \frac{1}{6}\left(\frac{15\pi}{16}\right)^{\frac{1}{3}}\left[\frac{C^{(6)}}{E}\right]^{1/3} \Big/ \theta^{4/3} \sin\theta \quad . \tag{II.6'}$$

Specializing for the L.-J.(12,6) potential, for which $C^{(6)} = 4\epsilon\sigma^6$ we obtain the low-angle reduced differential cross section:

$$I^*(\theta)^{(6)} \cong \frac{1}{6\pi}\left[\frac{15\pi}{4K}\right]^{1/3} \Big/ \theta^{4/3} \sin\theta \cong \frac{1}{6\pi}\left(\frac{15\pi}{4}\right)^{1/3} K^{-1/3}\,\theta^{-7/3} \quad . \tag{II.6''}$$

- - - - -

Thus a log-log plot of $\frac{d\sigma(\theta)}{d\Omega}$ or $I^*(\theta)$ vs. θ should exhibit linear limiting (low angle) behavior, with a slope of $-2(1+\frac{1}{s})$. Fig. 4 shows a log-log $I^*(\theta)$ plot corresponding to the example of Fig. 3. The continuously increasing positive deviation of $I^*(\theta)$ from the limiting behavior, out to the rainbow angle, is quite general for a realistic potential with a well.

Thus the influence of the short-range forces is most easily assessed by examining the angular dependence of the ratio $\frac{I^*(\theta)}{I^*(\theta)^{(6)}} \equiv \rho^*(\theta)$. Mason[3] has tabulated a function proportional to $\rho^*(\theta)$ for the Exp (α ,6) potential over a wide range of reduced collision energies. In Fig. 5 we see an example of $\rho^*(\theta)$ for a L.-J.(12,6) potential, corresponding to the case of Figs. 1-4.

Although the true total cross section (for reasons previously mentioned) is not determined within the classical framework, it is of interest to consider the incomplete total cross section, namely

$$\sigma(\theta_0) \equiv 2\pi \int_{\theta_0}^{\pi} \sin\theta \, \frac{d\sigma(\theta)}{d\Omega}\, d\theta \tag{a}$$

corresponding to the total cross section for scattering beyond some minimum angle θ_0 (usually the angular aperture or "resolving power" of an apparatus). Just as with the differential cross sections, no explicit analytical form can be obtained for $\sigma(\theta_0)$ in terms of the potential constants but, analogous to Eq. 6, an approximate form is available for the case of long-range inverse-power potentials. The energy dependence of these cross sections is the same as that of the differential cross sections (cf. Eq. 6). Tabulations of incomplete total cross section functions for the Exp (α, 6) potential are presented in Ref. 3.

Further information on various classical aspects of elastic molecular scattering theory may be found in Refs. 1-3, as well as in certain articles in a series by Amdur and co-workers[4] and elsewhere[5].

III. Resumé of Quantum Scattering Treatment[6]

The standard wave mechanical treatment of scattering by a central potential need not be elaborated here. It will suffice to define terms and outline the procedures required to predict the scattering amplitude and thus differential and total cross sections from an assumed potential.

Following Mott and Massey[6a], the scattering amplitude $f(\theta)$ is defined by the asymptotic equation for the amplitude function ψ of the colliding system (i.e., by the behavior of the wave function at large interparticle separation r):

$$\psi \sim e^{ikz} + f(\theta)\, e^{ikr}/r \tag{III.1}$$

where the z axis is the axial direction, θ the scattering angle and $k = \mu v_r/\hbar = 2\pi/\lambda = [2\mu E/\hbar^2]^{1/2}$ is the incident wave number (λ is the de Broglie wavelength). The differential cross section is given by

$$I(\theta) = |f(\theta)|^2 \tag{III.2}$$

and the total cross section by

$$Q = 2\pi \int_0^{\pi} \sin\theta \cdot |f(\theta)|^2 d\theta \ . \tag{III.3}$$

Using the Rayleigh - Faxen-Holtzmark method of partial waves (expanding $\psi = \sum_\ell R_\ell(r)\, P_\ell(\cos\theta)$, separating the wave equation, and following standard procedures) one finally obtains the (complex[*]) scattering amplitude expressed in terms of the phase shifts $\eta_\ell(k)$:

$$f(\theta) = \frac{1}{2ik} \sum_{\ell=0}^{\infty} (2\ell+1)(e^{2i\eta_\ell} - 1)\ P_\ell(\cos\theta) \tag{III.4a}$$

- - - - -

✱ In general, the scattering amplitude may be considered to be the sum of a real and an imaginary part: $f(\theta) = Re f(\theta) + Im f(\theta)$, where

$$Re f(\theta) = \frac{1}{2k} \sum_{\ell} (2\ell+1) \sin 2\eta_\ell\ P_\ell(\cos\theta) \tag{III.4b}$$

and

$$Im f(\theta) = \frac{1}{k} \sum_{\ell} (2\ell+1) \sin^2\eta_\ell\ P_\ell(\cos\theta) \tag{III.4c}$$

- - - - -

where ℓ is the orbital angular momentum quantum number, $P_\ell(\cos\theta)$ the Legendre function and η_ℓ the ℓth order phase shift, defined in terms of the asymptotic behavior of the ℓth order radial wave function $G_\ell(r) \equiv r R_\ell(r)$:

$$G_\ell(r) \sim \sin(kr - \ell\pi/2 + \eta_\ell) \propto e^{-i(kr - \ell\pi/2)} - e^{2i\eta_\ell} \cdot e^{i(kr - \ell\pi/2)} \tag{III.5}$$

where $G_\ell(r)$ is the solution of the radial equation

$$\left[\frac{d^2}{dr^2} + k^2 F(r)\right] G_\ell(r) = 0 \tag{III.6}$$

with the inner boundary condition $G_\ell(0) = 0$. Here

$$F(r) \equiv 1 - U(r)/k^2 - \ell(\ell+1)/k^2 r^2 \tag{III.7}$$

where $U(r) = \frac{2\mu}{\hbar^2} V(r)$. The phase shift η_ℓ thus refers to the displacement of the radial wave function, at large separations, relative to that of the corresponding ℓth order spherical Bessel function $j_\ell(kr)$. We note that $G_\ell^{\,0}(r) \equiv kr\, j_\ell(kr)$ represents what may be termed a "reference" radial function i.e., the solution of Eq. 6 in the absence of an interaction potential, V = 0 (with only the centrifugal potential term remaining). Thus $\eta_\ell = k \lim_{r\to\infty} \Delta r_z$ where Δr_z is the displacement of (the difference between) corresponding zeros of $G_\ell^{\,0}(r)$ and $G_\ell(r)$.

This definition of the phase shift is shown graphically in Fig. 6, in which the ordinate (y) is proportional to the radial wave function and the abscissa (x) is the reduced separation $x \equiv r/\sigma$, for a L.-J. potential. The displacement Δx (more properly, evaluated at very large x where the wave function is sinusoidal) yields directly the so-called "reduced phase"[2,6c] $\eta^* \equiv \eta/k\sigma$ introduced by Ford and Wheeler,[2] which is of considerable importance and will be discussed later.

For the particular case illustrated the phase shift is seen to be negative, corresponding to the domination of the repulsive branch of the potential. Thus, given any realistic potential function V(r), one solves (by numerical methods)[6c] the radial equation (Eq. 6) for successive values of ℓ, evaluating a sufficient number of phase shifts to obtain convergence (to some specified limit of accuracy) in the sum over ℓ in Eq. 4. For potentials with a long-range inverse-sixth power radial dependence it is found that $\eta_\ell \sim \ell^{-5}$ so that convergence presents no practical problem. The behavior of

the phases as a function of wave number for various realistic interaction potentials has been investigated in great detail[6c, 7-11] and will not be spelled out here. Fig. 1 displays a typical "smoothed curve" of η vs. ℓ . Plotted is η^* vs. $\beta \equiv (\ell+\frac{1}{2})/k\sigma$ for a L.-J. potential at one collision energy; later on we will identify this β with the reduced impact parameter $b^* = b/\sigma$ in connection with the semiclassical approximation[2,12].

For practical usage Eq. 2 may be rewritten in terms of real quantities only, as follows:

$$I(\theta) \equiv \frac{d\sigma(\theta)}{d\Omega} = \frac{1}{4k^2}\left\{\left[\sum_\ell (2\ell+1)\sin 2\eta_\ell \, P_\ell(\cos\theta)\right]^2 + \left[\sum_\ell (2\ell+1)(\cos 2\eta_\ell - 1) P_\ell(\cos\theta)\right]^2\right\} \qquad \text{(III.8)}$$

and Eq. (3) may be reduced using the orthogonality of the Legendre polynomials to yield the simple formula:

$$Q = \frac{4\pi}{k^2}\sum_\ell (2\ell+1)\sin^2\eta_\ell \qquad \text{(III.9)}$$

Calculated curves of $\frac{d\sigma(\theta)}{d\Omega}$ [and $Q(k)$] for various realistic potentials have appeared often in the literature[5c,6c,9-11]. Examples of $\frac{d\sigma(\theta)}{d\Omega}$ plots, for an L.-J. (12,6) potential, are shown in Figs 7 and 8. However, an alternative representation of a quantum-calculated angular distribution in the form $\rho^*(\theta)$ appears in Fig. 5. Suffice it to say that the differential cross sections show pronounced oscillatory (diffraction-like) behavior, with the periodicity, $\Delta\theta$, decreasing with increasing wave number. The total cross sections $Q(k)$ show a general decrease with increasing wave number, but often exhibit broad extrema (and, at very low energies

rather sharp resonances) for reasons to be discussed later. These non-classical features will be our main concern in the sections which follow.

IV. Approximation Methods

Although the exact quantum treatment of the elastic scattering problem (involving direct numerical integration of the radial wave equation as described in Sec. III) has been carried out in full on many occasions, suitable approximation methods have always been welcomed by workers in the field. In addition to easing the computational labor of evaluating wave functions, phase shifts and cross sections, the semiclassical approximation techniques nearly always add insight into the physics, often enabling certain qualitative inferences to be drawn and predictions to be made which would not be possible otherwise. In certain cases simple approximation formulas may be obtained which describe with good accuracy the main features of a particular quantum effect under consideration.

There are, however, various levels of approximation possible and these may be arranged in some sort of a hierarchy. In this section we shall consider, successively, approximations for

(a) the radial wave function, $G_\ell(r)$

(b) the phase shifts, $\eta_\ell(k)$

(i) phase shifts (no restriction on magnitude)

(ii) "small" phase shifts.

Succeeding sections will be concerned with approximations useful in regard to

(c) the scattering amplitude, $f(\theta)$

(d) the interference pattern in $I(\theta)$

(e) rainbow scattering, $I(\theta)$ near θ_r

(f) low-angle scattering, $I(\theta)$ for small θ

(g) the total cross section, $Q(v_r)$

a. The radial wave function.

The Jeffreys-WKBL approximation, recently designated[13] the "asymptotic approximation", AA, for the radial wave function is discussed in many texts; we will base our development here on the presentation of Landau and Lifshitz[14]. As is well known, the approximation is valid only in the limit of a very slowly-varying potential $(d \ln V(r)/dr \ll k_r)$, i.e., small enough de Broglie wavelength λ_r such that the fractional change in $V(r)$ over a wavelength is negligible. With this assumption the radial differential equation may be simplified and an approximate solution obtained in terms of the Airy function. The usual "semiclassical" radial wave functions are written in two forms expressing the asymptotic behavior on the two sides of the classical turning point r_0 (but not <u>at</u> the turning point itself, where $\lambda_r = \infty$):

$$G_\ell(r) \sim \begin{cases} \frac{1}{2}\left[\frac{p_\infty}{|p_r|}\right]^{1/2} \exp\left[-\frac{1}{\hbar}\int_{r_0}^{\infty} p_r\, dr\right], & (r<r_0) \quad \text{(IVa.1a)} \\ \left[\frac{p_\infty}{p_r}\right]^{1/2} \sin\left[\frac{1}{\hbar}\int_{r_0}^{\infty} p_r\, dr + \frac{\pi}{4}\right] & (r>r_0) \quad \text{(IVa.1b)} \end{cases}$$

Here $G_\ell(r)$ is the radial wave function normalized to unit asymptotic amplitude, p_r is the "local radial momentum" given by

$$p_r = \hbar k_r = h/\lambda_r = \left[2\mu\left(E - V_{eff}(r)\right)\right]^{1/2} \qquad \text{(IVa.2)}$$

with the effective potential (IVa.3)

$$V_{eff}(r) = V(r) + \left(\ell + \tfrac{1}{2}\right)^2 \hbar^2/2\mu r^2,$$

$p_\infty = \hbar k$ is the incident momentum,

$$k_r = k \cdot \left[F_c(r)\right]^{1/2} \tag{IVa.4}$$

is the local wave number,

$$F_c(r) = 1 - U(r)/k^2 - (\ell+\tfrac{1}{2})^2/k^2 r^2 = 1 - V(r)/E - b^2/r^2 = 1 - V_{eff}(r)/E \,, \tag{IVa.5}$$

$$b = (\ell+\tfrac{1}{2})/k \tag{IVa.6}$$

and the turning point is defined by the outermost zero of $F_c(r)$ i.e. $F_c(r_o) = 0$. (Note that the semiclassical $F_c(r)$ differs from the analogous quantum expression (Eq.III.7) in the centrifugal term where $(\ell+\frac{1}{2})^2$ replaces $\ell(\ell+1)$.

Although Eq. 1b suffices to evaluate the phase shifts (see below), the apparent singularity at the turning point as $p_r(r_o) = 0$ is a disadvantage for certain applications. Of course, this singularity is only an artifact due to the use of the asymptotic forms of the Airy integral. It may be removed by an alternate expansion of the Airy function around the turning point[15] which yields a satisfactory approximation for the wave function (effectively joining Eq. 1a with Eq. 1b) passing smoothly through the turning point.

The solution (valid for $-1 \leq z \leq 1$) may be represented by[15b]

$$G_\ell(r) = \left[\frac{k}{F_o'}\right]^{1/6} \cdot \pi^{1/2} \cdot \left[0.35503\,(1 - z^3/6) + 0.25882\, z\,(1 - z^3/12) + \cdots\right] \tag{IVa.7}$$

where $$z \equiv \left[\frac{F_o'}{k}\right]^{1/3} \cdot k \cdot (r - r_o)$$

(IVa.8

is the "reduced displacement" from the turning point and

$$F_0' = \left\{ \frac{d}{dr}\left[F_c(r)\right] \right\}_{r_0} \tag{IVa.9}$$

is proportional to the force at the turning point. The numerical coefficients arise from well-known expansion formulas for the Airy function. It is readily verified that Eq. (7) satisfies the Airy-like form of the radial equation near the turning point, and predicts quite accurately the position and amplitude of the first maximum in the wave function (which occurs very near $z = 1$). Beyond the first maximum, i.e., for $z > 1$, one may employ Eq. 1b, expressed here in a form suitable for numerical computation:

$$G_\ell(r) = \left[F_c(r)\right]^{-1/4} \sin\left[k \int_{r_0}^{r} \left[F_c(r)\right]^{1/2} dr + \pi/4 \right] \tag{IVa.10}$$

Thus the radial wave function may be approximated over the entire range $z \geq -1$ by the single expression

$$G_\ell(r) = (1-f)\left[\frac{k}{F_0'}\right]^{1/6} \cdot \left(0.6292 + 0.4588\, z - 0.1049\, z^3 - 0.0383\, z^4 + \cdots\right)$$

$$+ f \cdot \left[F_c(r)\right]^{-1/4} \sin\left[k \cdot (r_{eff} - r_0) + \pi/4 \right] \tag{IVa.11}$$

where $r_{eff} = \int_{r_0}^{r} \left[F_c(r)\right]^{1/2} dr$ and f is some "joining" or "mixing" function, for example $f = \left[1 + e^{-a(z-1)}\right]^{-1}$, with an <u>a</u> value of, say, 100, to effect rapid smoothing.

b. The phase shifts

(i) Phase shifts (no restriction on magnitude)

The JWKB-approximated phase shifts may be obtained directly from the asymptotic form of the AA radial wave function[6a,b,14]. Comparing the expressions

$$\sin\left[k\int_{r_0}^{R}[F_c(r)]^{1/2}dr + \pi/4\right] \tag{a}$$

and

$$\sin\left[kr - l\pi/2 + \eta_l\right] \tag{b}$$

in the limit of large R, we have

$$\eta_l = \lim_{R\to\infty}\left[k\int_{r_0}^{R}[F_c(r)]^{1/2}dr - kr\right] + \frac{\pi}{2}(l+\tfrac{1}{2})$$

$$= \frac{\pi}{2}(l+\tfrac{1}{2}) - kr_0 + k\int_{r_0}^{\infty}\left\{[F_c(r)]^{1/2} - 1\right\}dr \tag{IVb.1a}$$

where r_0 is the outermost zero of $F_c(r)$, as usual. For computational purposes Eq. 1 may be transformed to the form

$$\eta_l = \frac{\pi}{2}(l+\tfrac{1}{2}) + kr_0\left\{\int_0^1\left\{[F_c(y)]^{1/2} - 1\right\}\cdot y^{-2}dy - 1\right\} \tag{IVb.1b}$$

where $y \equiv r_0/r$. The pole in the integrand is readily dealt with by expanding around the origin, then integrating analytically from $y = 0 \to \varepsilon$ ($\varepsilon \ll 1$) and numerically from $\varepsilon \to 1$.

Since Eqs. 1 involve only a quadrature whereas the exact solution of the radial equation requires direct numerical integration of the second order differential equation, the AA phase shift calculation is faster by about two orders of magnitude. For energies high

enough (typically $K \equiv \frac{E}{\epsilon} \gtrsim 1$) so that there is no more than a single zero in F (r), i.e., above the critical energy for classical orbiting (or quantum mechanical tunneling through the centrifugal barrier), the AA phases are sufficiently accurate (ca. 0.1 per cent) for all but the most exacting practical applications. Except for the limitation that the absolute uncertainty (in radians) increases with the magnitude of η_ℓ (it is noted that for most purposes one requires η_ℓ modulo π with an accuracy of ca. 0.01 rad.), the JWKB approximation procedure imposes no restriction on the size of the phase shifts. In contrast, the Born approximation (mentioned below) is valid only for cases in which the phase shift is small (e.g. $\eta \lesssim \frac{1}{2}$ rad.) An alternative form of Eq. 1b is[6a,16].

$$\eta_\ell = k\left[\int_{r_0}^{\infty}\left[F_c(r)\right]^{1/2}dr - \int_{b}^{\infty}\left[F_c^{(0)}(r)\right]^{1/2}dr\right] \qquad \text{(IVb.1c)}$$

where $F_c^{(0)}(r) = 1-(\ell+\frac{1}{2})^2/k^2r^2$, i.e., the expression for F(r) in the absence of a potential, and b is its zero,

$$b = (\ell + 1/2)/k.$$

Still another semiclassical route to the phase shifts exists[18a] but discussion is best postponed to the next section (c).

(ii) "small" phase shift

When ℓ is sufficiently large (e.g. $\ell \gg kR$, where R is some "range" parameter of the potential) that the centrifugal term dominates the effective potential (Eq. 3), the wave function $G_\ell(r)$

approaches very closely the Bessel form, $G_\ell^{(0)}(r)$, and the phase shifts approach zero. Massey and Mohr[16a] showed that Eq. 1c could be simplified by suitably expanding $F_c(r)$ to yield the Jeffreys (J)-approximated phase

$$\eta_J \cong \frac{1}{2k}\int_b^\infty \frac{U(r)\,dr}{[F_c^{(0)}(r)]^{1/2}} = \frac{\mu}{\hbar^2 k}\int_b^\infty \frac{V(r)\,dr}{\left[1-\frac{(\ell+\frac{1}{2})^2}{k^2r^2}\right]^{1/2}} \qquad \text{(IVb.2a)}$$

so that for $V(r) \sim -C^{(s)}/r^s$

$$\eta_J^{(s)} = \frac{f(s)\mu C^{(s)}}{\hbar^2 k b^{s-1}} = \frac{f(s)C^{(s)}}{\hbar v b^{s-1}} = \frac{f(s)\mu C^{(s)}k^{s-2}}{\hbar^2(\ell+\frac{1}{2})^{s-1}} = a_s(\ell+\tfrac{1}{2})^{1-s} \qquad \text{(IVb.3)}$$

where $f(s) = \frac{1}{2}\pi^{1/2}\Gamma(\frac{1}{2}s-\frac{1}{2})/\Gamma(\frac{1}{2}s)$ (see p. 6) and a_s has an obvious meaning; of special interest is the coefficient $f(6) = 3\pi/16$. Massey and Smith[17] pointed out an alternative route to the higher order phases (Eqs. (2) and (3)) via the Born (B) approximation:

$$\eta_B \cong -\frac{\pi}{2}\int_0^\infty U(r)\left[J_{\ell+\frac{1}{2}}(kr)\right]^2 r\,dr = -k\int_0^\infty U(r)\,j_\ell^2(kr)\,r^2\,dr \qquad \text{(IVb.4)}$$

Making use of the fact that, for large ℓ, the main contribution to the integral arises from the region outside the first zero of the Bessel function, r_0 (where $r_0 \cong \ell/k$), and replacing the rapidly oscillatory part of the integrand by its mean value beyond r_0 (i.e., $\langle J^2_{\ell+\frac{1}{2}}(x)\rangle = \frac{1}{\pi x}\cdot(1-\ell^2/x^2)^{-1/2}$) one obtains

$$\eta_B \cong -\frac{1}{2k}\int_b^\infty \frac{U(r)\,dr}{(1-\ell^2/k^2r^2)^{1/2}} \cong -\frac{1}{2k}\int_b^\infty \frac{U(r)\,dr}{[F_c^{(0)}(r)]^{1/2}} = \eta_J \equiv \eta_{JB} \qquad \text{(IVb.2b)}$$

For an (asymptotic) inverse sixth power potential, the Jeffreys-Born (JB) approximation for the higher-order phases may be written:

$$\eta^{(6)}_{JB} = \frac{3\pi}{16}\frac{\mu C^{(6)}}{\hbar^2}\cdot\frac{k^4}{(\ell+\frac{1}{2})^5} = \frac{3\pi}{16}\frac{C^{(6)}}{\hbar v}\cdot b^{-5} \qquad \text{(IVb, 5)}$$

where $\ell + 1/2$ may often be replaced by ℓ. For sufficiently large ℓ (e.g., for $\ell \gg kR$, or, at least $\ell > L$ such that $\eta(L) \lesssim \frac{1}{2}$) the accuracy of the JB approximation is adequate (e.g., $\pm$ 0.01 rad.) for most applications.[*]

- - - - -

[*] For an L.-J. (12,6) potential, Eq. 5 may be re-written[6c, 18]

$$\eta_{JB} = \frac{3\pi}{8}\frac{BA^4}{(\ell+\frac{1}{2})^5} \quad \text{or} \quad \eta^*_{JB} \equiv \frac{\eta_{JB}}{A} = 3\pi/(8K\beta^5)$$

where $A \equiv k\sigma$, $B \equiv 2\mu\epsilon\sigma^2/\hbar^2$, $K \equiv A^2/B = E/\epsilon$ and $\beta \equiv \frac{\ell+\frac{1}{2}}{A} = \frac{b}{\sigma} = b^*$.

- - - - -

V. The Scattering Amplitude[2,6ab]

Ford and Wheeler[2] extended the Mott-Massey[6a] semiclassical treatment of the scattering amplitude to yield practical approximation formulas for $f(\theta)$. In the present discussion we shall recapitulate the relevant material and develop certain new relations especially suitable for molecular scattering applications.

Starting with the exact expression, Eq. III.4, for the scattering amplitude, restricting θ to the region $\varepsilon \leq \theta \leq \pi - \varepsilon$ (where ε is an infinitesimal angle), making use of the relation

$$\sum_{\ell} (2\ell+1) P_\ell(\cos\theta) = 0 \qquad (\theta \neq 0, \pi) \tag{V.1}$$

and the Laplace expansion for the Legendre function for large ℓ , (valid for $\sin\theta \gtrsim 1/\ell$):

$$P_\ell(\cos\theta) \sim \left(\frac{2}{\pi \ell \sin\theta}\right)^{1/2} \cdot \sin\left[(\ell+\tfrac{1}{2})\theta + \tfrac{\pi}{4}\right] = \frac{i}{(2\pi\ell\sin\theta)^{1/2}} \left\{ e^{-i(\frac{\pi}{4}+(\ell+\frac{1}{2})\theta)} - e^{i(\frac{\pi}{4}+(\ell+\frac{1}{2})\theta)} \right\} \tag{V.2}$$

we replace the sum by an integral over ℓ , use ℓ in place of $\ell+\frac{1}{2}$ and obtain directly the expression:

$$f(\theta) \cong \frac{-1}{k(2\pi\sin\theta)^{1/2}} \cdot \int_0^\infty d\ell \cdot \ell^{1/2} \cdot \left[e^{iB_1(\ell)} - e^{iB_2(\ell)} \right] \tag{V.3}$$

where

$$B_1(\ell) \equiv 2\eta_\ell + \ell\theta + \pi/4$$

and

$$B_2(\ell) \equiv 2\eta_\ell - \ell\theta - \pi/4 \ . \tag{V.4}$$

Since the terms in the integrand are rapidly oscillating and will for the most part, destructively interfere, it is appropriate to use the method of stationary phase[19]. Here we seek values of ℓ , say L,

for which one or the other of the B's are stationary, e.g., $(B_1')_L \equiv \left(\frac{dB_1}{dl}\right)_L = 0$; the only significant contribution to the integral arises from the regions near the L's. Setting $B_1' = 0$ (Eq. 4) we have $\eta_L' = -\frac{1}{2}\theta_L$; for the condition $B_2' = 0$, $\eta_L' = \frac{1}{2}\theta_L$ where $\eta_L' \equiv \left(\frac{d\eta}{dl}\right)_L$. Referring back to Part II on the classical deflection function, we recall that for net repulsive deflections $\theta \equiv \Theta > 0$, while for net attractive trajectories $\theta \equiv -\Theta > 0$ (see also Fig. 1a, top). Thus for the contributions from the "attractive" branch of the deflection function we have $\eta_L' = \frac{1}{2}\Theta_L$, corresponding to $B_1' = 0$, i.e., domination of the B_1 term in Eq. 3. For the contribution from the "repulsive" branch we have, <u>also</u>, $\eta_L' = \frac{1}{2}\Theta_L$, corresponding to $B_2' = 0$, and thus domination of the B_2 term. The general relation applicable over the entire range of the deflection function is thus:

$$\eta_L' = \frac{1}{2}\Theta_L \quad ; \tag{V.5}$$

it is known as the semiclassical equivalence relationship.*

- - - - -

* Eq. 5 may be utilized[18a] for phase shift evaluation by integration:

$$\eta_L = \frac{1}{2}\int_L^\infty \Theta\, dl = \frac{k}{2}\int_b^\infty \Theta\, db \tag{V.5'}$$

or

$$\eta^* = \frac{1}{2}\int_\beta^\infty \Theta\, d\beta \tag{V.5''}$$

where the notation is the same as that used previously. Eq. 5" is in a convenient form for the calculation of reduced phases from already -

available deflection functions. The accuracy attainable is the same as that of Eqs. IVb.1a or IVb.1c. It is noted from Eq. 5" that η attains its maximum value at $\beta = \beta_m = b_0 \sigma$ (cf. Fig. 1b bottom).

- - - - -

Returning now to Eq. 3, we follow through with the stationary phase procedure. Anticipating somewhat the final result, we can express $f(\theta)$ as the sum of the three (possible) contributions from the two branches of the deflection function:

$$f(\theta) = f_a(\theta) + f_b(\theta) + f_c(\theta)$$

where a,b and c refer (see Figs 1 and 2) to the three regions of ℓ (or impact parameter) corresponding (by the stationary phase principle) to the specified angle θ. Here a refers to the outermost attractive one, b to the inner attractive one and c to the inner repulsive one. Of course, if $\theta > \theta_r$ (where θ_r is the rainbow angle) there will be only one region of stationary phase, i.e., near c; however, we will retain the three terms for generality.

For each region, we expand $B(\ell)$ around the stationary values

$$B(\ell) = B(L) + \tfrac{1}{2} B''_L \cdot (\ell - L)^2 + \tfrac{1}{6} B'''_L \cdot (\ell - L)^3 + \cdots \quad , \quad \text{where}$$

$$B''_L \equiv \left[d^2 B(\ell)/d\ell^2 \right]_L = 2\eta''_L \quad , \quad \text{etc.}$$

Thus (for $\theta < \theta_r$) there will be two stationary values, say L_a and L_b, for the B_1 term and one, L_c, for the B_2 term. Considering first the contribution of the outermost term, $f_a(\theta)$, we require evaluation of the integral involving B_1 in Eq. 3. Removing the stationary quantities from the integral we obtain

$$f(\theta) \cong \frac{-1}{k(2\pi\sin\theta)^{1/2}} \cdot \int_0^\infty dl \cdot l^{1/2} \cdot e^{iB_1(L_a)} e^{\frac{i}{2}B_L''\cdot(l-L_a)^2} = -\frac{1}{k}\left[\frac{L_a}{2\pi\sin\theta}\right]^{1/2} e^{iB_1(L_a)} \cdot J \tag{V.6a}$$

where

$$J \equiv \int_0^\infty dl \cdot e^{i\eta_{La}''(l-L_a)^2} \cong \int_{-\infty}^\infty dx \cdot e^{i\eta_{La}''\cdot x^2}, \quad \text{with } x \equiv l - L_a . \tag{V.6b}$$

For this case, a, $\eta_{La}'' > 0$ so that \20a/

$$J = \left(\frac{\pi}{\eta_{La}''}\right)^{1/2} \cdot e^{i\pi/4} . \tag{V.7}$$

Making use of Eq. 4, we obtain

$$\begin{aligned} f_a(\theta) &= -\frac{1}{k}\cdot\left[\frac{L_a}{2\eta_{La}''\cdot\sin\theta}\right]^{1/2} \cdot e^{i(2\eta_{La} + L_a\theta + \pi/2)} \\ &= \frac{1}{k}\cdot\left[\frac{L_a}{2\eta_{La}''\cdot\sin\theta}\right]^{1/2} \cdot e^{i(2\eta_{La} + L_a\theta - \pi/2)} \equiv Ae^{iB} \end{aligned} \tag{V.8}$$

Thus $\mathrm{Re}\, f_a(\theta) = A\cos B$ and $\mathrm{Im}\, f_a(\theta) = A\sin B$; the ratio of the real to the imaginary part of the amplitude is thus $\mathrm{Re}\, f_a(\theta)/\mathrm{Im}\, f_a(\theta) = \cot B = \cot(2\eta_{La} + L_a\theta - \pi/2)$; $\theta \neq 0, \pi$.

For the inner attractive contribution, b, $\eta_{Lb}'' < 0$ and thus \20b/

$$J = \left(\frac{\pi}{-\eta_{Lb}''}\right)^{1/2} \cdot e^{-i\pi/4} \tag{V.9}$$

so that

$$\begin{aligned} f_b(\theta) &= -\frac{1}{k}\cdot\left[\frac{L_b}{2(-\eta_{Lb}'')\sin\theta}\right]^{1/2} \cdot e^{i(2\eta_{Lb} + L_b\theta)} \\ &= \frac{1}{k}\left[\frac{L_b}{2(-\eta_{Lb}'')\cdot\sin\theta}\right]^{1/2} \cdot e^{i(2\eta_{Lb} + L_b\theta - \pi)} \end{aligned} \tag{V.10}$$

For the repulsive contribution, $f_c(\theta)$ is given by the analog of Eq. 6 with B_2 in place of B_1. However, $\eta_{Lc}'' < 0$, so J is of the form (9). Thus we obtain

$$f_c(\theta) = \frac{1}{k}\cdot\left[\frac{L_c}{2(-\eta_{Lc}'')\cdot\sin\theta}\right]^{1/2} \cdot e^{i(2\eta_{Lc} - L_c\theta - \pi/2)} . \tag{V.11}$$

Combining Eqs. (8), (10) and (11) we obtain

$$f(\theta) = \frac{1}{k(2\sin\theta)^{1/2}}\left\{\left(\frac{L_a}{\eta''_{La}}\right)^{1/2} e^{i(2\eta_{La}+L_a\theta-\frac{\pi}{2})} + \left(\frac{L_b}{-\eta''_{Lb}}\right)^{1/2} e^{i(2\eta_{Lb}+L_b\theta-\pi)} + \left(\frac{L_c}{-\eta''_{Lc}}\right)^{1/2} e^{i(2\eta_{Lc}-L_c\theta-\pi/2)}\right\} \qquad (\theta \neq 0, \pi) \qquad \text{(V.12)}$$

such that $I(\theta) = |f(\theta)|^2$. Utilizing the semiclassical equivalence relationship, with $L_a \cong k b_{La}$, we note that the quantity $(L_a/\eta''_{La})^{1/2}$ becomes $k\left[2b/\frac{d\theta}{db}\right]^{1/2}$, where $\frac{d\theta}{db}$ is the slope of the deflection function at $b = b_{La}$. Similar expressions result at L_b and L_c.

Recalling the classical relation $I_i(\theta) = \frac{b_i}{\sin\theta\left|\frac{d\theta}{db_i}\right|}$ (cf. Eq. 3 of Sec. II) it is seen that each of the three terms in Eq. 12 is of the proper form

$$f_i(\theta) = \left[I_i(\theta)\right]^{1/2} e^{i\gamma_i} \qquad \text{(V.13)}$$

(where γ_i is a phase factor) such that $I_i(\theta) = |f_i(\theta)|^2$. However, there will be interference among the three terms, which will yield a non-classical angular distribution.

For later applications (Sec. IX) it will be of interest to consider the limiting form of Eq. 12 for small angles, $\sin\theta \cong \theta$). Referring to Fig. 1 it is seen that for small angles the two inner regions coalesce, i.e., $L_b \cong L_c \equiv L_o$, $\eta_{Lb} \cong \eta_{Lc} \cong \eta_{max} \equiv \eta_m$, $\eta'_{Lb} \cong \eta'_{Lc} \cong 0$, and $\eta''_{Lb} \cong \eta''_{Lc} \equiv \eta''_o$.
Thus the contribution of the last two terms of Eq. 12 may be approximated by

$$f_{bc}(\theta) \cong \frac{1}{k}\left[\frac{L_0}{2(-\eta_0'')\theta}\right]^{1/2} e^{i(2\eta_m - \frac{3\pi}{4})} \cdot \left[e^{i(L_0\theta - \frac{\pi}{4})} + e^{-i(L_0\theta - \frac{\pi}{4})}\right]$$

$$= \frac{2}{k}\left[\frac{L_0}{2(-\eta_0'')\theta}\right]^{1/2} e^{i(2\eta_m - \frac{3\pi}{4})} \cdot \cos(L_0\theta - \pi/4) \tag{V.14a}$$

$$\cong 2\left[I_{bc}(\theta)\right]^{1/2} e^{i\gamma_m} \cdot \cos(L_0\theta - \pi/4)$$

where $I_{bc}(\theta) = b_0 / \sin\theta \cdot \left|\frac{d\Theta}{db}\right|_{b_0}$ (V.14b)

is the classical contribution from branch b (<u>or</u> c), and $\gamma_m = 2\eta_m - \frac{3\pi}{4}$ is the phase factor. Recalling the classical result (noting that $\left|\frac{d\Theta}{db}\right|_{b_{La}} \ll \left|\frac{d\Theta}{db}\right|_{L_0}$, i.e., that $I_a(\theta) \gg I_b(\theta) + I_c(\theta)$ for small angles, we incorporate Eq. 14 into Eq. 12 and express $f(\theta)$ for small angles in terms of the dominant long-range part:

$$f(\theta) \cong \left[I_a(\theta)\right]^{1/2} e^{i\gamma_a} \cdot \left\{1 + 2\left[\frac{I_{b,c}(\theta)}{I_a(\theta)}\right]^{1/2} e^{i(\gamma_m - \gamma_a)} \cdot \cos(L_0\theta - \pi/4)\right. \tag{V.15}$$

where

$$\gamma_a \equiv 2\eta_{La} + L_a\theta - \pi/2 .$$

The origin of the interference effects in the angular distribution (e.g., Figs. 5,7-9) is now apparent.

VI. The Interference Pattern

For simplicity we restrict the present discussion to angles $\lesssim 30^\circ$ (for which we may replace $\sin\theta$ by θ). From Eq. V.15 we obtain the following expression for the differential cross section, provided, of course, that $\theta < \theta_r$:

$$I(\theta) = I_a(\theta)\left\{1 + [Y(\theta)]^2 + 2Y(\theta)\cdot\cos\gamma(\theta)\right\} \tag{VI.1}$$

where
$$Y(\theta) \equiv 2\left[\frac{I_{b,c}(\theta)}{I_a(\theta)}\right]^{1/2}\cdot\cos\left(L_0\theta - \frac{\pi}{4}\right) \equiv Y_{max}(\theta)\cdot\cos\left(L_0\theta - \frac{\pi}{4}\right) \tag{VI.2}$$

and
$$\gamma(\theta) \equiv \gamma_m - \gamma_a = 2(\eta_m - \eta_{La}) - L_a\theta - \pi/4 \tag{VI.3}$$

Since $I_a(\theta) = I(\theta)^{(6)}$, Eq. 1 may be re-written to yield the desired ratio $\rho^*(\theta)$:

$$\rho^*(\theta) = 1 + Y(\theta)^2 + 2Y(\theta)\cos\gamma \tag{VI.4}$$

The main factor governing the interference pattern in $\rho^*(\theta)$ or $I(\theta)$ is that involving $Y(\theta)\cdot\cos\gamma$; since $2\frac{I_{b,c}}{I_a} < 1$ for moderately small angles (i.e., θ not too close to θ_r), the Y^2 term is of lesser importance. The oscillatory product may be expressed

$$\cos\left(L_0\theta - \frac{\pi}{4}\right)\cdot\cos\gamma(\theta) = \frac{1}{2}\left\{\cos\left[-\theta(L_a - L_0) + 2(\eta_m - \eta_{La}) - \pi/2\right] + \cos\left[\theta(L_a + L_0) - 2(\eta_m - \eta_{La})\right]\right\}. \tag{VI.5}$$

From this equation one sees that the "wavelengths" in the pattern of $\rho^*(\theta)$ are $2\pi/|L_a - L_o|$ and $2\pi/(L_a + L_o)$. The shorter of the two wavelengths is designated $\Delta\theta$. Thus

$$\Delta\theta = 2\pi/(L_a + L_o) \tag{VI.6}$$

is the angular spacing between successive minima (or maxima) in the oscillatory function $\rho^*(\theta)$. This is, for practical purposes, the same as the corresponding spacing in $I(\theta)$. It is noted that this spacing is not independent of angle; since L_a decreases with an increase in θ (see Fig. 1), the spacing $\Delta\theta$ increases with θ.

Fig. 9 shows an example of a complicated interference pattern in $\rho^*(\theta)$, calculated* for a L.-J. (12,6) potential. The curves refer to one specified reduced collision energy K, with various assumed values of the wavenumber parameter A (or, alternately stated, for different values of the quantum parameter $\Lambda^* \equiv \frac{\hbar}{\sigma(2\mu\epsilon)^{1/2}} = \frac{2\pi}{B^{1/2}} = \frac{2\pi K^{1/2}}{A}$).

- - - - -

* The calculations were made via the semiclassical (AA) phase shifts (Eq. 1b of Sec. IVb) and the exact summation formula for $I(\theta)$ (Eq. 8 of Sec. III)

- - - - -

For a given K, the deflection function $\Theta(\beta)$ is fully determined (and thus also the classical differential cross section), so differences due purely to quantum effects are clearly displayed. As expected, the periodicity of the oscillations decreases with increasing wavenumber. Re-writing Eq. 6, we see that

$$A\,\Delta\theta = 2\pi/(\beta_{\theta a} + \beta_m) \tag{VI.7}$$

for any given K. Figs. 10 shows an analysis of the interference pattern of Fig. 9 (and of other similar curves at the same K), according to Eq. 7. The agreement between spacings predicted (Eq. 7) and computed (from $\rho^*(\theta)$ curves) is nearly within the accuracy of the latter determinations, except for a few low angle points.

Next we consider the amplitude of the oscillations in $\rho^*(\theta)$. Eq. 2 shows that $Y(\theta)$ is governed by the classical intensity ratio $I_{b,c}(\theta)/I_a(\theta)$ or, alternatively expressed, by the classical $\rho^*(\theta)$, which is determined solely by K. Thus the amplitude is expected to be independent of the wavenumber or the quantum parameter. According to Eq. 2 the maximum value allowed for $Y(\theta)$ is

$$Y_{max}(\theta) = \sqrt{2}\left[\frac{2\,I_{b,c}(\theta)}{I_a(\theta)}\right]^{1/2} = \sqrt{2}\left[\rho^*_{cl}(\theta) - 1\right]^{1/2} \tag{VI.8}$$

where $\rho^*_{cl}(\theta)$ is the classical value of $\rho^*(\theta)$. (The minimum value for $Y(\theta)$ is, of course, $-Y_{max}(\theta)$.)

From Eq. 4, $\rho^*(\theta)$ is bounded by

$$\left[1 + Y_{max}(\theta)\right]^2 \geq \rho^*(\theta) \geq \left[1 - Y_{max}(\theta)\right]^2 \tag{VI.9}$$

or

$$\left\{1 + \sqrt{2}\left[\rho^*_{cl}(\theta) - 1\right]^{1/2}\right\}^2 \geq \rho^*(\theta) \geq \left\{1 - \sqrt{2}\left[\rho^*_{cl}(\theta) - 1\right]^{1/2}\right\}^2 \tag{VI.10}$$

It is found that Eq. 10 predicts quite well the envelope of the oscillations (i.e., the limits on the oscillation amplitude) for the examples of Figs. 5 and 9.

Inspection of Fig. 9 shows, in addition, a very important

implication of Eq. 10, i.e., the overall independence of the amplitude upon wavenumber (or quantum parameter). Thus, provided $\theta < \theta_r$, i.e., three terms contributing to the amplitude, we see that while the angular spacing $\Delta\theta$ decreases smoothly to zero with increasing wavenumber (or decreasing quantum parameter) at constant K, the amplitude of the quantum interferences (oscillations) remains <u>finite</u> in the classical limit ($\Lambda^* = 0$). Experimentally, however, small velocity inhomogeneities would tend to mask the oscillations when $\Delta\theta$ becomes too small.

Following upon Eq. 13 in Sec. IV.c, we have restricted our discussion to small angles ($\theta \lesssim 30^\circ$), but there is no difficulty in generalizing Eq. 13 slightly to include the larger angle cases provided, of course, that $\theta < \theta_r$, by keeping the f_b and f_c terms separate. The smallest angular spacing between minima, $\Delta\theta$, then becomes $2\pi/(L_a + L_b)$. Eq. 10 for the amplitude of $\rho^*(\theta)$ should still be approximately correct, with $\rho^*_{cl}(\theta) = 1 + \frac{I_b(\theta) + I_c(\theta)}{I_a(\theta)}$. The conclusion of the last paragraph about the persistence of the amplitude of the quantum effect is not altered.

However, for angles appreciably beyond the rainbow angle ($\theta > \theta_r$) only one branch of the deflection function contributes to f(θ); i.e., $f_b(\theta) \cong f_c(\theta) \cong 0$. Thus the quantum oscillations rapidly damp out in the classical limit. This is the same behavior as that expected for any monotonic potential (the deflection function $\Theta(b)$ is also monotonic) in which case $I(\theta) = |f_a(\theta)|^2 \cong I_{cl}(\theta)$ (cf. Eq. 13); a familiar example is that of scattering by the rigid sphere potential[16b].

The discussion of this section thus confirms the remark by Ford and Wheeler[2] that there exists the possibility of deducing information regarding the phase angles in the scattering amplitude by observing interference of waves scattered out of more than one part of the incident wave front. Experiments showing these interference effects have recently been carried out[21].

VII. Rainbow Scattering[2]

Ford and Wheeler[2] (FW) applied the semiclassical method to the calculation of the rainbow scattering amplitude for the general case, where Θ_r may be either positive or negative. In the present connection, i.e., for the atomic and molecular scattering problem, Θ_r and thus $(d\eta/dl)_{l_r}$ are invariably negative; $(d^2\eta/dl^2)_{l_r} = \frac{1}{2}\left(\frac{d\Theta}{dl}\right)_{l_r} = 0$ by definition of the rainbow condition and $(d^3\eta/dl^3)_{l_r} = \frac{1}{2}(d^2\Theta/dl^2)_{l_r} \equiv q$ is always positive. For this special case it seems worthwhile to re-derive and amend the FW results, retaining the notation of the previous sections.

The scattering amplitude near the rainbow angle can be expressed

$$f(\theta) = f_a(\theta) + f_b(\theta) + f_c(\theta) = f_r(\theta) + f_c(\theta) \qquad \text{(VII.1)}$$

where f_a and f_b have been combined to give the rainbow contribution to the aplitude, f_r. The repulsive contribution $f_c(\theta)$ is given by

$$f_c(\theta) = \left[I_c(\theta)\right]^{1/2} \cdot e^{i\gamma_c} \qquad \text{(VII.2)}$$

where $\gamma_c = 2\eta_{L_c} - L_c\theta - \pi/2$, as in Sec. V. To evaluate f_r, associated with the attractive branch of the deflection function, we must make use of the function B_1 of Eq. V.4. Expanding η_l in the neighborhood of the rainbow angle we find

$$\eta_l = \eta_r - \frac{1}{2}\theta_r \cdot (l - l_r) + \frac{1}{6} q \cdot (l - l_r)^3 \qquad \text{(VII.3)}$$

This is accomplished by making use of the expansion

$\Theta = \cancel{\Theta_r + \frac{1}{2}\left(\frac{d^2\Theta}{d\beta^2}\right)_{\beta_r}} = \Theta_r + q\cdot(l - l_r)^2$ and noting that

$\theta = -\theta_r$. The fact that $\eta''_{l_r} = 0$ makes it necessary to extend the stationary phase treatment of Sec. V to include the cubic terms in Eq. 3.

Thus

$$B_1 = 2\eta_r - \theta\cdot(l-l_r) + \tfrac{1}{3}q\cdot(l-l_r)^3 + l\theta + \frac{\pi}{4} \equiv B_1(l_r) + \Delta B_1 \qquad \text{(VII.4)}$$

where

$$B_1(l_r) \equiv 2\eta_r + l_r\theta_r + \pi/4$$

and

$$\Delta B_1 = \tfrac{1}{3}q\cdot(l-l_r)^3 + (\theta-\theta_r)\cdot(l-l_r) + l_r\cdot(\theta-\theta_r)$$

so that

$$f_r(\theta) \cong -\frac{1}{k}\left[\frac{l_r}{2\pi\sin\theta}\right]^{1/2}\cdot e^{iB_1(l_r)}\int_{-\infty}^{\infty} e^{i\Delta B_1}\cdot d(l-l_r)$$

$$= -\frac{1}{k}\left[\frac{l_r}{2\pi\sin\theta}\right]^{1/2}\cdot e^{i(2\eta_r + l_r\theta + \frac{\pi}{4})}\int_{-\infty}^{\infty} e^{i\left[\frac{q}{3}(l-l_r)^3 + (\theta-\theta_r)(l-l_r)\right]}\, d(l-l_r)$$

$$= \frac{1}{k}\cdot\left[\frac{l_r}{2\pi\sin\theta}\right]^{1/2}\cdot e^{i\delta}\, q^{-1/3}\, 2\pi\, Ai(x) = \left[I_r(\theta)\right]^{1/2} e^{i\delta} \qquad \text{(VII.5)}$$

where $\delta \equiv 2\eta_r + l_r\theta - 3\pi/4$, $x \equiv q^{-1/3}(\theta-\theta_r)$, Ai(x) is the Airy function, and $I_r(\theta) = |f_r(\theta)|^2$. (The above result (correct) for the phase angle δ differs by $-\pi/2$ from that quoted by FW.)

Thus $$f(\theta) \cong \left[I_c(\theta)\right]^{1/2} e^{i\gamma_c} + \left[I_r(\theta)\right]^{1/2} e^{i\delta} \qquad \text{(VII.6)}$$

and $$I(\theta) \cong I_c(\theta) + I_r(\theta) + 2\left(I_c\, I_r\right)^{1/2}\cos(\delta - \gamma_c) \qquad \text{(VII.7)}$$

where $$I_r(\theta) = \frac{1}{k^2}\cdot\frac{2\pi l_r}{\sin\theta}\cdot q^{-2/3}\cdot Ai^2\left[q^{-1/3}(\theta-\theta_r)\right].$$

Since the principal maximum of Ai(x) occurs for $x \cong -1$, $I_r(\theta)$ achieves it largest value at an angle significantly smaller than the rainbow angle, namely, where $\theta = \theta_r - q^{1/3}$. As pointed out by FW, the low-resolution rainbow "peak" is spread out over an appreciable angular range and under no conditions (i.e., even at high k) approximates the classical sharp "spike" in the differential cross section at $\theta = \theta_r$.

The interference pattern near the rainbow angle is given by Eq. 7. The differential cross section oscillates between the limits $I_{max}(\theta)$ and $I_{min}(\theta)$ where

$$I_{max}(\theta) = \left[I_r^{1/2} + I_c^{1/2}\right]^2$$

and

$$I_{min}(\theta) = \left[I_r^{1/2} - I_c^{1/2}\right]^2 \tag{VII.8}$$

with a periodicity governed by $\delta - \gamma_c$. Analogous to the treatment in Sec. V (which yielded Eq. V.6) we obtain for the "wavelength" of the oscillations in the neighborhood of the broad rainbow maximum:

$$\Delta\theta = \frac{2\pi}{\frac{d}{d\theta}(\delta - \gamma_c)} = \frac{2\pi}{l_r + L_c} \quad . \tag{VII.9}$$

As one progresses to angles appreciably larger than the rainbow angle the amplitude of the oscillations decreases and eventually the nearly monotonic behavior characteristic of single-branch (non-interfering) scattering obtains. On the low angle side of the rainbow, the three contributions (from the two branches of the deflection function) always produce interference, as discussed in Sec. V.

It is of some interest to note that published results of direct (numerical) computations[6c,9b,21a] of $I(\theta)$ employing the full phase shift treatment for monoenergetic scattering by a L.-J.(12,6) potential have not displayed distinct rainbow maxima which show through the oscillatory pattern (cf. Fig. 7). However, for values of the quantum parameter Λ^* smaller than about 0.1, the expected effect appears, quite pronounced.

There is now ample experimental confirmation of the rainbow scattering phenomenon in atomic and molecular systems via beam scattering studies in three laboratories[22]. As originally pointed out by Mason[3], measurements of the energy dependence of θ_r make possible in a rather direct way the evaluation of the potential well depth ϵ for any assumed functional form of the interaction potential. Suitable calculations of rainbow angle vs. K have now been made for the L.-J.(12,6)[1a,22a], Exp(α, 6)[2,23], Kihara[23] and Morse[24,25] potential functions.

The related "tunneling-orbiting" phenomenon has also received a certain amount of attention[2] but the subject has not yet been fully developed and, for reasons of brevity, will not be treated here.

VIII. Low-Angle Scattering[26]

Massey and Mohr[16b,27] (MM) first considered the problem of the limiting form of the low angle behavior of the differential scattering cross section according to quantum mechanics. It was found that for any potential falling off faster than r^{-2}, $I(\theta)$ and thus Q is finite. They also introduced the so-called random-phase (rph) approximation, which is especially applicable to the practical heavy-particle case in which a great many phase shifts are required in the sums for the cross sections. Since most of these phases are large (compared to π) and only principal values of the angles are relevant, they (the η_ℓ's) may be considered to be essentially random numbers, for $0 \leq \ell \leq L$. The upper limit, L, may be estimated fairly accurately for the rigid-sphere case; here $L \cong kr_o$, where r_o is the rigid-sphere diameter.

Eq. III.8 may be expressed as

$$I(\theta) = \frac{1}{4k^2}\left\{\left[\sum_\ell (2\ell+1)\sin 2\eta_\ell \cdot P_\ell(\cos\theta)\right]^2 + \left[\sum_\ell (2\ell+1)\cdot 2\sin^2\eta_\ell \cdot P_\ell(\cos\theta)\right]^2\right\} \qquad \text{(VIII.1)}$$

With the random-phase assumption (strictly valid only in the rigid-sphere case in the limiting case of very high wavenumber i.e., $kr_o \gg 1$) the first term is negligible compared with the second due to the extensive cancellation in the oscillating $\sin 2\eta_\ell$ term. In the limit $\theta \cong 0$, upon replacing all terms in $P_\ell(\cos\theta)$ by 1, we obtain

$$I(0) \cong \frac{1}{k^2}\left[\sum_\ell (2\ell+1)\sin^2\eta_\ell\right]^2 = \left(\frac{kQ}{4\pi}\right)^2 \qquad \text{(VIII.2)}$$

(making use of the expression for Q which has been given in Eq. III.9). The quantity $\left(\frac{kQ}{4\pi}\right)^2$ will be designated $I(0)_{rph}$ hereafter. Removing the average value of $\sin^2\eta_l$ (i.e., $\langle \sin^2\eta_l \rangle_{rph} = \frac{1}{2}$) we obtain for the rigid sphere case the well-known result

$$I(0) \cong \frac{1}{k^2}\left[\frac{1}{2}\sum_{l=0}^{L}(2l+1)\right]^2 = \frac{(L+1)^4}{4k^2} \cong \frac{1}{4}k^2 r_0^4 \qquad \text{(VIII.3)}$$

and

$$Q \cong 2\pi r_0^2 \qquad \text{(VIII.4)}$$

For backscattering, i.e., $\theta = \pi$, with $P_l(-1) = (-1)^l$ we find

$$I(\pi) \cong \frac{1}{k^2}\left[\frac{1}{2}\sum_{l=0}^{L}(2l+1)(-1)^l\right]^2 = \frac{(L+1)^2}{4k^2} \cong \frac{1}{4}r_0^2 \qquad \text{(VIII.5)}$$

which is the classical result for the differential cross section (classically the scattering would be isotropic with $I(\theta) = \frac{1}{4}r_0^2$ for all θ). The strong, non-classical forward peak (Eq. 3), known as the diffraction or shadow scattering contribution, increases in magnitude with increasing k but is confined to smaller and smaller angles (i.e., $\theta < \theta^*$, where θ^* is the limiting angle) as k is increased[16b]; here $\theta^* \cong \pi/kr_0$. Making use of this, Massey and Mohr[16b] showed that the shadow scattering contributes (approximately) a constant amount, namely πr_0^2, to the total cross section of $2\pi r_0^2$ (Eq. 4).

Employing the rph-approximation and taking advantage of the expansion of $P_l(\cos\theta)$ at small angles, they proposed[27] that the low angle differential scattering cross section was of an exponential form. It will be instructive to derive here the limiting ($\theta \to 0$)

functional form of $I(\theta)$ within the framework of the random-phase approximation.

As noted in Sec. III. the scattering amplitude consists of a real and an imaginary part

$$\mathrm{Re}\, f(\theta) = \frac{1}{2k} \sum_{l} (2l+1) \sin 2\eta_l \; P_l(\cos\theta) \tag{VIII.6}$$

$$\mathrm{Im}\, f(\theta) = \frac{1}{k} \sum_{l} (2l+1) \sin^2 \eta_l \; P_l(\cos\theta) \tag{VIII.7}$$

[It is noted that for the random-phase case (i.e., $\langle \sin 2\eta_l \rangle_{rph} = 0$) Re $f(\theta) = 0$; thus the scattering amplitude is pure imaginary and $I(\theta) = [\mathrm{Im}\, f(\theta)]^2$]

Setting $\theta = 0$ and comparing Eq. 7 with Eq. III.9 we obtain the very important general result (known as the optical theorem).

$$Q = \frac{4\pi}{k} \mathrm{Im}\, f(0) \tag{VIII.8}$$

from which we derive the useful inequality:

$$|\mathrm{Re}\, f(0)| = \left[I(0) - \left(\frac{kQ}{4\pi}\right)^2 \right]^{1/2} = \left[I(0) - I(0)_{rph} \right]^{1/2} \geq 0 \; . \tag{VIII.9}$$

Thus the (extrapolated) forward differential scattering cross section $I(0)$ may never be <u>less</u> than $(kQ/4\pi)^2$. This allows a (partial) consistency check on experimental measurements of low angle differential cross sections and independently-obtained (e.g., via attenuation measurements) total cross sections.

It is convenient to define a dimensionless "forward scattering ratio"

$$j(k) \equiv \frac{I(0)}{I(0)_{rph}} = 1 + \left[\frac{\mathrm{Re}\, f(0)}{\mathrm{Im}\, f(0)} \right]^2 \geq 1 \; . \tag{VIII.10}$$

It is seen that the quantity $(j-1)^{1/2} = Re\,f(0)/Im\,f(0)$ is a measure of the deviation from the rph-approximation condition. In general, the fractional part of the forward intensity due to the real part of $f(\theta)$ is

$$[Re\,f(0)]^2/I(0) = (j-1)/j \qquad \text{(VIII.11)}$$

(with $j = 1$ implying zero for the real part of the forward amplitude).

Fig. 11 shows a graph of $j(kr_0)$ for the rigid sphere potential compared to the L.-J. (12,6) potential (for a specified value of the parameter B). It is seen that <u>even in the rigid sphere case</u> at $A \equiv kr_0 \cong 25$ (i.e., $r_0/\lambda \cong 4$), the ratio Re f(0): Im f(0) is significantly greater than zero (<u>ca</u> 1:5) while for the L.-J. potential it may exceed 1:1.

The undulatory behavior in j(A) is characteristic of a realistic interaction potential with a minimum (an attractive well); the origin of the extrema will be discussed in the next section. It will suffice here to call attention to the fact that the velocity dependence of the forward scattering should show such extrema, with the magnitude of the "excess" in j indicating the fractional contribution of the real part of the forward scattering amplitude which originates from the "non-random" phases.

Continuing with the rph-approximation, the low-angle differential cross section is readily evaluated by expanding the Legendre polynomial and replacing the sum over ℓ by an integral as usual. Thus we obtain:

$$I(\theta) = [\mathrm{Im}\, f(\theta)]^2 = \left[\frac{1}{k}\int_0^L 2\ell \cdot \frac{1}{2} \cdot \left(1 - \frac{\ell^2\theta^2}{4} + \frac{\ell^4\theta^4}{64} - \cdots\right) d\ell \right]^2$$

$$\cong \frac{L^4}{4k^2} \cdot \left[1 - \frac{\theta^2 L^2}{8} + \frac{\theta^4 L^4}{192} - \cdots \right]^2$$

$$= I(0)_{rph} \cdot \left[1 - \left(\frac{k^2 Q \theta^2}{8\pi}\right) + \frac{1}{2}\left(\frac{k^2 Q \theta^2}{8\pi}\right)^2 \cdot \frac{5}{6} - \cdots \right]$$

$$\cong I(0)_{rph} \cdot \exp\left[- k^2 Q \theta^2 / 8\pi \right] \tag{VIII.12}$$

where we have made use of Eqs. 2 and 3, i.e., $L^2 \cong k^2 Q/2\pi$ and approximated the series $1 - x + \frac{x^2}{2} \cdot \frac{5}{6} - \cdots$ by e^{-x}, for $x \ll 1$. For low angle scattering by a <u>rigid sphere</u> potential, replacing $I(0)_{rph}$ by $I(0)\left[= j \cdot I(0)_{rph}\right]$, we have

$$I(\theta) = j(kr_0) \cdot \left(\frac{kQ}{4\pi}\right)^2 \cdot \exp\left[- k^2 Q \theta^2 / 8\pi \right], \tag{VIII.13}$$

with $j(kr_0) \to 1$ and $Q \to 2\pi r_0^2$ in the "classical" limit. For this limiting case, as a check, we estimate the contribution ΔQ to the total cross section $Q\,(= 2\pi r_0^2)$ from the strong shadow scattering peak, assuming the exponential approximation for $I(\theta)$ to be valid out to θ^*:

$$\Delta Q = \int_0^{\theta^*} 2\pi\, I(\theta) \sin\theta\, d\theta \cong 2\pi\, I(0)_{rph} \int_0^{\theta^*} \theta \exp\left[-k^2 Q \theta^2 / 8\pi \right] d\theta$$

$$= \frac{8\pi}{k^2 Q} \cdot I(0)_{rph} \left[1 - e^{-\frac{k^2 Q \theta^{*2}}{8\pi}} \right] \cong \frac{Q}{2} \cdot (0.92) \cong \pi r_0^2 \tag{VIII.14}$$

as expected.

Next we reconsider the important problem of low angle scattering by an inverse-power potential of the form $V(r) = -C^{(s)}/r^s$ In connection with his measurements of small-angle scattering, Pauly[26a] derived an approximate expression (via the Massey-Mohr technique) for the differential cross section at low angles, for an inverse sixth-power potential. He obtained

$$I(\theta) = j(\theta) \cdot I(0)_{rph} \exp\left[-c\left(k^2 Q\, \theta^2/8\pi\right)\right] \qquad \text{(VIII.15)}$$

with $c = 2.08$ and $j = 1.36$. The latter implies via Eq. 10 a large and constant ratio of the real to be imaginary part of the forward amplitude, $\mathrm{Re}\, f(0)/\mathrm{Im}\, f(0) = 0.6$; it is large because of the many small and slowly-varying high-order phase shifts associated with this long-range potential. The factor c in the exponent is to be compared to unity for the rph case; it originates from this same source. Helbing and Pauly[26b,c] and Mason et al.[26d] have independently repeated and refined the derivation, extending it to the general case ($s > 5$). Their results are in excellent agreement. For the special case of $s = 6$, they obtained $j = 1.525$ and $c = 2.07$. (This value of j supersedes the less reliable, earlier value quoted above. It yields a still higher real component to the forward amplitude; the ratio $\mathrm{Re}\, f(0)/\mathrm{Im}\, f(0) = 0.725$.)

We now outline the derivation of the general case, following along the lines of Ref. 26d. For the potential above, the higher-order phase shifts are given by

$$\eta^{(s)}_{JB} \cong a_s\, \ell^{1-s} \qquad \text{(VIII.16a)}$$

where

$$a_s = f(s)\mu C^{(s)} k^{s-2}/\hbar^2 \qquad \text{(VIII.16b)}$$

according to Eq. IV.b.3.

Expanding the Legendre (here we carry only first order terms), and simplifying as usual, Eq. (1) may be written:

$$I(\theta)^{(s)} \cong \frac{4}{k^2}\left\{\left[J_1 - \frac{\theta^2}{4}J_2\right]^2 + \frac{1}{4}\left[J_3 - \frac{\theta^2}{4}J_4\right]^2\right\} \qquad \text{(VIII.17a)}$$

where

$$J_1 \equiv \int_0^\infty dl\, l \sin^2\eta_l , \qquad J_2 \equiv \int_0^\infty dl\, l^3 \sin^2\eta_l ,$$

$$J_3 \equiv \int_0^\infty dl\, l \sin 2\eta_l , \quad \text{and} \quad J_4 \equiv \int_0^\infty dl\, l^3 \sin 2\eta_l . \qquad \text{(VIII.17b)}$$

Factoring out the most important quantities, we may express $I(\theta)^{(s)}$ in terms of the key integral J_1 and various ratios of integrals:

$$I(\theta)^{(s)} \cong \frac{4}{k^2} J_1^2 \left\{\left[1 - \frac{\theta^2}{4}\frac{J_2}{J_1}\right]^2 + \frac{1}{4}\left(\frac{J_3}{J_1}\right)^2\left[1 - \frac{\theta^2}{4}\cdot\frac{J_4}{J_3}\right]^2\right\} \qquad \text{(VIII.18)}$$

Before proceeding, we note that J_1 is closely related to the imaginary part of the forward amplitude and thus to the total cross section. From the definition of J_1 and Eq. 7 (replacing the sum by an integral over l as usual), we deduce the relations

$$J_1 = \frac{k}{2}\,\mathrm{Im}\, f(0) = k^2 Q/8\pi . \qquad \text{(VIII.19)}$$

To evaluate the integrals J_1-J_4 exactly would require an accurate knowledge of η_l for all l. We may circumvent this by following the suggestion of Landau and Lifshitz[28] to replace η_l by η_{JB} throughout, since the principal contribution to the integrals

arises from the higher-order phases in any case. All the J integrals may be put into a common standard form; the results may be summarized as follows:

$$J_1 = a^{\frac{2}{s-1}} / G(s), \quad \text{where} \quad G(s) \equiv \frac{1}{\pi} \cdot 2^{\frac{3s-5}{s-1}} \cdot \sin\left(\frac{\pi}{s-1}\right) \cdot \Gamma\left(\frac{2}{s-1}\right) \tag{VIII.20a}$$

$$\frac{J_2}{J_1} = (2a)^{\frac{2}{s-1}} \cdot \frac{\frac{1}{2}\sin\left(\frac{\pi}{s-1}\right) \cdot \Gamma\left(\frac{2}{s-1}\right)}{\sin\left(\frac{2\pi}{s-1}\right) \cdot \Gamma\left(\frac{4}{s-1}\right)} = J_1 \cdot \frac{2}{\pi} \tan\left(\frac{\pi}{s-1}\right) \cdot \frac{\left[\Gamma\left(\frac{2}{s-1}\right)\right]^2}{\Gamma\left(\frac{4}{s-1}\right)} \tag{VIII.20b}$$

$$\frac{J_3}{J_1} = \left(\frac{4}{s-1}\right) \cdot \frac{\sin\left(\frac{\pi}{s-1}\right) \cdot \Gamma\left(\frac{2}{s-1}\right)}{\sin\left(\frac{\pi}{2} \cdot \frac{s+1}{s-1}\right) \cdot \Gamma\left(\frac{s+1}{s-1}\right)} = 2 \tan\left(\frac{\pi}{s-1}\right) \tag{VIII.20c}$$

$$\frac{J_4}{J_3} = (2a)^{\frac{2}{s-1}} \cdot \frac{\frac{1}{2}\cos\left(\frac{\pi}{s-1}\right) \cdot \Gamma\left(\frac{2}{s-1}\right)}{\cos\left(\frac{2\pi}{s-1}\right) \cdot \Gamma\left(\frac{4}{s-1}\right)} = J_1 \cdot \frac{2}{\pi} \cdot \tan\left(\frac{2\pi}{s-1}\right) \cdot \frac{\left[\Gamma\left(\frac{2}{s-1}\right)\right]^2}{\Gamma\left(\frac{4}{s-1}\right)} \tag{VIII.20d}$$

Thus

$$I(\theta)^{(s)} \cong \frac{4}{k^2}\left(\frac{k^2 Q}{8\pi}\right)^2 \left\{ \left[1 - \frac{k^2 Q}{16\pi} f_1(s)\, \theta^2\right]^2 + \tan^2\left(\frac{\pi}{s-1}\right) \left[1 - \frac{k^2 Q}{16\pi} f_2(s)\, \theta^2\right]^2 \right\} \tag{VIII.21}$$

where, following Mason et al.[26d] we have defined

$$f_1(s) = \frac{1}{\pi} \tan\left(\frac{\pi}{s-1}\right) \cdot \frac{\left[\Gamma\left(\frac{2}{s-1}\right)\right]^2}{\Gamma\left(\frac{4}{s-1}\right)} \tag{VIII.22a}$$

and

$$f_2(s) = \frac{1}{\pi} \tan\left(\frac{2\pi}{s-1}\right) \cdot \frac{\left[\Gamma\left(\frac{2}{s-1}\right)\right]^2}{\Gamma\left(\frac{4}{s-1}\right)} \quad . \tag{VIII.22b}$$

Squaring terms in Eq. 21, and dropping only terms involving θ^4, we obtain finally

$$I(\theta)^{(s)} \cong \left(\frac{kQ}{4\pi}\right)^2 \left[1 + \tan^2\left(\frac{\pi}{s-1}\right)\right] \cdot \left[1 - \frac{1}{2} f_2(s) \frac{k^2 Q\, \theta^2}{8\pi}\right] . \tag{VIII.23}$$

Mason et al.[26d] retained the terms in θ^4 and then replaced the quantity in the second bracket by the exponential, yielding a result which may be expressed in our "standard form"

$$\frac{I(\theta)^{(s)}}{I(0)_{rph}} \cong j(s) \exp\left[-c(s)\,\frac{k^2 Q}{8\pi}\,\theta^2\right] \qquad \text{(VIII.15'; VIII.24a)}$$

with*

$$j(s) = 1 + \tan^2\left(\frac{\pi}{s-1}\right)$$

and

$$c(s) = \frac{1}{2\pi}\tan\left(\frac{2\pi}{s-1}\right)\cdot\frac{\left[\Gamma\left(\frac{2}{s-1}\right)\right]^2}{\Gamma\left(\frac{4}{s-1}\right)}\ ; \quad c(6) = 2.07. \qquad \text{(VIII.24b)}$$

- - - - -

*It is noted that this result for j is velocity-independent whereas even for the rigid sphere potential (cf. Fig. 11) j varies with kr_0, only approaching constancy (unity) as $\lambda/r_0 \to 0$. This is due to the significant fractional contribution of the non-random, higher order phases even in this case; however, their relative importance decreases with increasing kr_0.

- - - - -

Here we see that for the inverse s th power potential, $\mathrm{Re}\, f(0)/\mathrm{Im}\, f(0) = \tan\left(\frac{\pi}{s-1}\right)$. Thus the ratio approaches zero as $s \to \infty$ (i.e., the rigid sphere case).

Helbing and Pauly's[26c] result is identical with Eq. 24; however, they express the relationship slightly differently; they also introduce an angle θ_s^* such that the exponential may be expressed as $\exp\left[-\left(\frac{\theta}{\theta_s^*}\right)^2\right]$; thus for s = 6, $\theta^* = \dfrac{1.965}{k\left(\frac{Q}{\pi}\right)^{1/2}}$.

Fig. 12 shows a typical plot[26d] of the low angle differential cross section according to Eq. 24. The important quantum feature is the leveling off of the differential cross section to a finite value as $\theta \to 0$. This yields, of course, a finite total cross section (in contrast to the classical infinite result) as required; this will be discussed further in the next section.

IX. Glory Interference Effect at Low Angles

For a realistic, non-monotonic potential the classical deflection function $\Theta(b)$ will always pass through zero at a finite value of the impact parameter, say b_o; if the collision energy is low enough it may also go through $-\pi$, -2π, etc.[1] Classically (Eq. II.3), whenever $\sin\Theta = 0$ (provided $d\theta/db$ is finite) a pole (or "glory"[2]) occurs in the scattering at the appropriate angle (zero for a forward glory, 180° for a backward glory).

For simplicity we consider here only the forward glory, which is always found (at all energies) in the scattering by a realistic potential. Fig. 1 shows a typical deflection function with the glory impact parameter $b_o = \beta_m \sigma$ while Fig. 2 illustrates the effect on the differential cross section in a graphical way: one notes the vertical tangent (dB/dC) at $C = 1$ (i.e. $\theta = 0$) for $B = \frac{1}{2\pi}\beta_m^2$. Thus there are two classical contributions to the divergence in the forward scattering, one from very large impact parameters ($b \to \infty$) and the other from the glory impact parameter. Quantum mechanically these interfere, so we must add amplitudes rather than intensities, as discussed in Sec. V. In this section we elaborate further on this glory interference, with particular attention to its energy-dependence.

Ford and Wheeler[2] first developed an expression for the glory amplitude, making use of the stationary phase approximation. We will re-derive their result and combine it with Eq.V.8 for $f_a(\theta)$, the "outer attractive" contribution to the amplitude. This will yield an equation (essentially, Eq. VI.1) for the low angle scattering which correctly takes into account the important forward glory

contribution for a realistic potential. It therefore supersedes Eq. VIII.24a, intended to apply only to a monotonic (r^{-s}) potential. The oscillatory behavior of the forward scattering ratio j(k) (pointed out in the previous section) is a direct consequence of the glory contribution to the low angle scattering.

The derivation of FW is spelled out for a backward glory, while we choose here to deal specifically with the forward glory effect and its interference with the long-range contribution to the low angle scattering.

Returning to the treatment of Sec. V, we note that in the present application the Laplace expansion for the Legendre polynomial is not valid, since $\theta \lesssim \ell^{-1}$. We employ, therefore, one of the expansions in terms of the Bessel function, for example, that of Hilb[29]

$$P_\ell(\cos\theta) \sim \left(\frac{\theta}{\sin\theta}\right)^{\frac{1}{2}} J_0\left[(\ell+\tfrac{1}{2})\theta\right] \cong J_0(\ell\theta) \qquad \text{(IX.1)}$$

valid for large ℓ and small θ. Here J_0 is the zero-order Bessel function,

$$J_0(\ell\theta) = \int_0^{2\pi} \exp(i\ell\theta\cos\phi)\, d\phi/2\pi \quad . \qquad \text{(IX.2)}$$

In the neighborhood of the maximum phase (or the "glory phase"), designated $\eta_m(\beta_m)$ or $\eta_m(L_0)$, we expand η (to the quadratic term only

$$\eta = \eta_m + \tfrac{1}{2}\eta_m''\cdot(\ell - L_0)^2 \qquad \text{(IX.3a)}$$

where

$$\eta_m'' = \left[\frac{d^2\eta}{d\ell^2}\right]_{L_0} = \frac{1}{2}\left[\frac{d\Theta}{d\ell}\right]_{L_0} = \frac{1}{2\lambda}\left[\frac{d\Theta}{d\beta}\right]_{\beta_m} < 0 \, . \qquad \text{(IX.3b)}$$

Then, upon making the usual approximations, and proceeding as before, using Eqs. V.6b and 9, we obtain the glory amplitude

$$f_g(\theta) \cong \frac{e^{2i\eta_m}}{ik} \cdot L_0 \cdot J_0(L_0\theta) \cdot \int_{-\infty}^{\infty} e^{i\eta''_m \cdot (l-L_0)^2} \, d(l-L_0)$$

$$= \frac{1}{k}\left[\frac{\pi}{-\eta''_m}\right]^{1/2} L_0 \cdot J_0(L_0\theta)\, e^{i(2\eta_m - \frac{3\pi}{4})} = \left[I_g(\theta)\right]^{1/2} e^{i\gamma_m} \qquad \text{(IX.4a)}$$

where $\gamma_m \equiv 2\eta_m - 3\pi/4$

and $$I_g(\theta) \equiv \frac{\pi L_0^2}{k^2(-\eta''_m)} \cdot \left[J_0(L_0\theta)\right]^2 \cong I_g(0)\left[1 - \frac{L_0^2\theta^2}{2} + \cdots\right] \qquad \text{(IX.4b)}$$

with $I_g(0) \equiv \frac{\pi}{(-\eta''_m)} \cdot \frac{L_0^2}{k^2}$. The above expansion of J_0 is useful only for very small angles*: $\theta \lesssim l^{-1}$. Eq. 4a yields the important results:

$$\mathrm{Im}\, f_g(0) = \left[I_g(0)\right]^{1/2} \sin(2\eta_m - 3\pi/4) \qquad \text{and} \qquad \text{(IX.5a)}$$

$$\mathrm{Re}\, f_g(0) = \left[I_g(0)\right]^{1/2} \cos(2\eta_m - 3\pi/4) \,. \qquad \text{(IX.5b)}$$

We also recall (from Eq. VIII.7) that for the long range (outer attractive) contribution,

$$\mathrm{Im}\, f_a(0) \cong \frac{2}{k}\int_0^{\infty} dl\, l \sin^2\eta_{JB} = \frac{2}{k} \cdot J_1 \qquad \text{(cf Eq. (VIII.17b)} \qquad \text{(IX.5c)}$$

- - - - -

* In Eq. 4b the Bessel function has been expanded in order to display the angular dependence of the glory scattering at very low angles; however, for $\theta \gtrsim l^{-1}$ this development is no longer valid and the sinusoidal expansion is to be used:

$$J_0(L_0\theta) \sim \left(\frac{2}{\pi L_0\theta}\right)^{1/2} \cos(L_0\theta - \pi/4) \qquad \text{(IX.6)}$$

so that $f_g(\theta) = \frac{1}{k}\left[\frac{2L_0}{-\eta''_m}\right]^{1/2} \cdot \cos\left(L_0\theta - \frac{\pi}{4}\right) e^{i\gamma_m}$, (IX.7)

identical with Eq. V.14, obtained in a very slightly different way. Thus

$$I(\theta) = I_a(\theta)\left\{1 + 2\left[\frac{L_0}{L_a}\frac{\eta''_{La}}{(-\eta''_m)}\right]^{1/2} e^{i(\gamma_m - \gamma_a)} \cdot \cos\left(L_0\theta - \frac{\pi}{4}\right)\right\} , \quad \text{(IX.8)}$$

the same as Eq. V.15; the discussion of the interference effects in Sec. VI follows .

- - - - -

In Sec. VI the interference pattern in the angular distribution arising from the glory effect has been analyzed in detail, but an important feature was intentionally omitted and reserved for the present discussion, namely, the energy-dependence (or velocity-dependence) of the forward scattering.

We have seen in Sec. VIII that j(s), the forward scattering ratio for an inverse-s power potential is independent of k (Eq. VIII, 24b): $j(s) = 1 + \tan^2\left(\frac{\pi}{s-1}\right)$, so that $Im\, f(0)/Re\, f(0) = \cot\left(\frac{\pi}{s-1}\right)$ = Const.) However, considering the glory contribution (alone), this ratio is seen to be $\tan\left(2\eta_m - \frac{3\pi}{4}\right)$, fluctuating from zero (pure positive real) when $\eta_m(k) = \frac{3}{8}\pi$ to ∞ (pure positive imaginary) when $\eta_m(k) = \frac{5}{8}\pi$, to zero again (pure positive real) when $\eta_m(k) = \frac{7}{8}\pi$ and to $-\infty$ (pure negative imaginary) when $\eta_m(k) = \frac{9}{8}\pi$, etc. Thus for a non-monotonic, realistic potential the forward scattering ratio should show an oscillatory velocity dependence (cf. Fig. 11). The practical implications of this conclusion will be discussed in Sec. XI.

X. Total Elastic Cross Section[10a]

Massey and Mohr[16a] were the first to develop an approximation formula (in closed form) for the total elastic cross section appropriate for heavy-particle scattering according to an inverse sth power potential. The usual cross section sum (Eq. III.4) was broken up into two parts $Q_{MM} = Q_< + Q_>$, corresponding to two broad regions of angular momentum, the first $(0 \leq \ell \leq L)$ in which the phase shifts are large and essentially random, where the rph-approximation is applicable, and the second ($\ell > L$) where they are small (but non-random) and for which the JB-approximation is valid. The division was arbitrarily made at $\ell = L$ such that $|\eta_{JB}(L)| = \frac{1}{2}$; the result fortunately does not depend very strongly on the choice of the cut-off phase in the neighborhood of, say, $\pi/4$. We shall now outline briefly the MM treatment.

For the rph region, as usual, the sum is found directly:

$$Q_< \cong \frac{8\pi}{k^2} \sum_{\ell=0}^{L} (\ell + \tfrac{1}{2}) \cdot \tfrac{1}{2} \cong \frac{2\pi L^2}{k^2} \tag{X.1}$$

while for the JB-region we have

$$Q_> \cong \frac{8\pi}{k^2} \int_L^\infty d\ell\, (\ell + \tfrac{1}{2}) \sin^2 \eta_{JB} \cong \frac{8\pi}{k^2} \int_L^\infty d\ell\, \ell \eta_{JB}^2 \tag{X.2}$$

(replacing $\ell + \frac{1}{2}$ by ℓ , the sum by an integral and $\sin \eta_{JB}$ by η_{JB} for $|\eta_{JB}| \leq \frac{1}{2}$). Substituting for η_{JB} from Eq. VIII.16a (or Eq. IV.b3) we obtain

$$Q_> \cong \frac{4\pi}{k^2} \frac{a_s^2}{(s-2)} \cdot L^{4-2s} \cong \frac{\pi}{(s-2)} \frac{L^2}{k^2} \tag{X.3a}$$

where we have utilized the cut-off condition to determine L:

$$L = \left[2\cdot|a_s|\right]^{\frac{1}{s-1}} = \left[\frac{2\mu C^{(s)}}{\hbar^2}\cdot k^{s-2}\cdot f(s)\right]^{\frac{1}{s-1}} \quad . \tag{X.3b}$$

As expected, $Q_<$ dominates; the ratio $Q_> : Q_<$ is only 1:(2s-4). Thus the MM cross section becomes

$$Q_{MM} = \frac{\pi}{k^2}\cdot L^2\cdot\left(\frac{2s-3}{s-2}\right) = \pi\left(\frac{2s-3}{s-2}\right)\cdot\frac{(2a_s)^{\frac{2}{s-1}}}{k^2} \quad . \tag{X.4}$$

Substituting for a_s from Eq. VIII.16b, we obtain directly

$$Q_{MM} = p_{MM}(s)\cdot\left[C^{(s)}/\hbar v\right]^{\frac{2}{s-1}} \tag{X.5a}$$

where*

$$p_{MM}(s) \equiv \pi\left(\frac{2s-3}{s-2}\right)\cdot\left[2f(s)\right]^{\frac{2}{s-1}} \quad . \tag{X.5b}$$

- - - - -

* Typical values of the dimensionless parameter $p_{MM}(s)$ are[10a] 10.613, 7.547, 7.062, 6.771, and 6.296 for s = 4, 6, 7, 8 and 12 respectively.

- - - - -

A somewhat more accurate[10a] approximation treatment is that of Landau and Lifshitz[28], in which the entire Q sum is replaced by an integral, and JB phases are used throughout (cf. sec. VIII. Eqs. 17)

Thus $$Q_{LL} = \frac{8\pi}{k^2}\int_0^\infty dl\, l \sin^2\eta_{JB} = \frac{8\pi}{k^2}\cdot J_1 \tag{X.6}$$

where J_1 is the same as that of Sec. VIII (evaluated in Eq. VIII.20a).

Analogous to Eq. 4 above, we find that

$$Q_{LL} = \pi^2 (2a_s)^{\frac{2}{s-1}} \Big/ \sin\left(\frac{\pi}{s-1}\right) \cdot \Gamma\left(\frac{2}{s-1}\right) \tag{X.7}$$

or

$$Q_{LL} = \mathcal{P}_{LL}(s) \cdot \left[C^{(s)}/\hbar v \right]^{\frac{2}{s-1}} \tag{X.8a}$$

where*

$$\mathcal{P}_{LL}(s) \equiv \pi^2 \left[2 f(s)\right]^{\frac{2}{s-1}} \Big/ \sin\left(\frac{\pi}{s-1}\right) \cdot \Gamma\left(\frac{2}{s-1}\right) . \tag{X.8b}$$

- - - - -

*Typical values of $\mathcal{P}_{LL}(s)$ are[10a] 11.373, 8.083, 7.529, 7.185, and 6.584 for $s = 4, 6, 7, 8$ and 12, respectively.

- - - - -

An identical expression for the total cross section results[10a] from the application of still another approximation procedure, namely, that of Schiff[30]. It has been found[10a] that the Schiff-Landau-Lifshitz (SLL) approximation formula for Q yields results in good agreement with calculations involving direct summation based on exact phase shifts.

The SLL approximation may also be obtained immediately via the optical theorem, making use of Eqs. VIII.19 and 20a for $\mathrm{Im}\, f(0)$ (and, of course, Eq. VIII.16b for a_s): $Q = \frac{4\pi}{k} \mathrm{Im}\, f_a(0) = \frac{8\pi}{k^2} \cdot J_1$, yielding Q_{SLL} directly.

For the important case of $s = 6$ (London dispersion) we have

the result:

$$Q^{(6)}_{SLL} = 8.083 \cdot \left[C^{(6)}/\hbar v \right]^{2/5} . \tag{X.9}$$

This implies yhat a log-log plot of Q(v) should be linear with a slope of -2/5. This monotonic velocity dependence would be expected to be applicable to the total cross sections for scattering of neutrals (atoms or molecules) in the thermal energy range, provided the influence of the short-range exchange and repulsive forces can be neglected. That this is not the case[6c,31] will shortly become apparent (see below).

One possible source of deviation in the behavior of the total cross section for elastic scattering of neutrals at thermal velocities from that predicted by Eq. 9 is the neglect of the induced dipole-quadrupole and retardation terms in the long-range potential. By a direct extension of the rph technique, simple approximation formulas have been derived[32] for the (separate) dipole-quadrupole and retardation effects upon Q .

Assuming a potential of the form

$$V(r) \sim -\frac{C^{(6)}}{r^6}\left(1 + \beta/r^2\right) \tag{X.10}$$

the fractional correction on Q_{SLL} (Eq. 9) is found to be

$$\frac{\Delta Q}{Q} \cong \frac{2\pi}{3}\frac{\beta}{Q} \tag{X.11}$$

For a retarded potential, given approximately by the expression

$$V(r) \sim -\frac{C^{(6)}}{r^6} \cdot \left(\frac{a}{a+r}\right) \tag{X.12}$$

where a is closely related to the "retardation wavelength" .

the fractional correction may be shown to be

$$\frac{\Delta Q}{Q} \cong -Q^{1/2}/a\pi^{3/2} \quad . \tag{X.13}$$

These deviations are small (for most systems of interest) and opposite in sign. For typical atomic systems in the thermal energy region the <u>net</u> deviation ranges from about -5 to + 10 per cent, becoming more positive with increasing relative velocity.

XI. Extrema in Total Cross Sections[31]

We have already noted (Secs. V and IX) that for a realistic potential possessing a minimum the classical deflection function $\Theta(b)$ passes through zero at the glory impact parameter b_o. Thus the phase shift curve $\eta(\ell)$ exhibits a broad maximum around $\eta_m(L_o)$, providing a significant fraction of non-random phases at intermediate angular momenta. The maximum phase, η_m, increases with a decrease in k, and, if the attractive well is deep enough, $\eta_m(k)$ can pass successively through multiples of $\pi/2$, giving rise alternately to positive and negative incremental contributions, $\frac{\Delta Q}{Q}$, to the rph-approximated (MM) total cross section. Thus Q(v) should display an undulatory velocity dependence (cf. Fig. 13), with the positions (and magnitudes) of the extrema determined primarily by $\eta_m(k)$ [and $\eta''_m(k)$]. For any given potential one may evaluate the dependence upon wave number of η_m (and η''_m), either by direct or indirect methods, and thus predict the extrema-velocities and extrema-amplitudes. With an assumed functional form for the potential, certain parameters of the potential may thus be deduced from experimental observations of this type.

The first quantitative treatment[31] of the extrema effect, following its original prediction[6c], employed a MM-type semiclassical analysis. This yielded as a condition for an extremum the relation

$$\eta_m(k_N) = (N - \tfrac{3}{8})\pi \qquad \text{(XI.1)}$$

where N = 1, 2, 3, ... are indices for maxima (while N = 1.5, 2.5, 3.5,... refer to minima) in the deviation function

$\frac{\Delta Q}{\bar{Q}} = [Q - Q^{(6)}]/Q^{(6)}$ vs. k or v. Fig. 14 shows an example of such a deviation function for a L.-J. (12,6) potential of specified parameters. A simpler and more exact derivation of the deviation function $\frac{\Delta Q}{\bar{Q}}$ was later derived by Düren and Pauly[33], making use of a SLL-type approximation and taking advantage of the optical theorem (Sec. VIII). We shall briefly outline their procedure and present the results.

Combining Eqs. VIII. 8, 19 and IX.5 we obtain the cross section as the sum of the usual (SLL) long-range outer attractive term and an additional glory term:

$$Q = \frac{4\pi}{k}\cdot\left[\mathrm{Im}\, f_a(0) + \mathrm{Im}\, f_g(0)\right] = \frac{4\pi}{k}\left(\frac{2J_1}{k}\right) + \frac{4\pi}{k}\left[I_g(0)\right]^{1/2}\cdot \sin\left(2\eta_m - \frac{3\pi}{4}\right)$$

$$= Q_{SLL} + \Delta Q \qquad \text{(XI.2a)}$$

where

$$\Delta Q = \frac{4\pi L_0}{k^2}\left[\frac{\pi}{-\eta_m''}\right]^{1/2}\cdot \sin\left(2\eta_m - 3\pi/4\right) \qquad \text{(XI.2b)}$$

Thus ΔQ is an oscillatory function of $\eta_m(k)$; note that $\langle \Delta Q \rangle = 0$ and $\langle Q \rangle = Q_{SLL}$. Maxima in the deviation function $\frac{\Delta Q}{\bar{Q}}$ occur when $2\eta_m - \frac{3\pi}{4} = \frac{\pi}{2}, \frac{5\pi}{2}$, etc. Thus the condition for an extremum may be expressed, as before.

$$\eta_m(k_N) = \pi\cdot\left(N - \frac{3}{8}\right) \qquad \text{(XI.1)}$$

where indices N = 1,2,3,... define maxima; N = 1.5, 2.5, 3.5... correspond to minima (as mentioned earlier).

Eq. 10 is quite general and indicates that it is possible to

evaluate the maximum in the phase shift curve, η_m, and its energy dependence directly from observed extrema in Q (v).

The amplitude of the oscillation in $\Delta Q/\bar{Q}$ is (from Eq. 2b)

$$U \equiv \frac{|\Delta Q|_{max}}{\bar{Q}} = \frac{4\pi L_0}{k^2 \bar{Q}} \left[\frac{\pi}{-\eta_m''}\right]^{1/2} = \frac{4\beta_m}{\bar{Q}} \cdot \left[\frac{2\pi}{-\Theta_m' \cdot A}\right]^{1/2} \tag{XI.3}$$

where the usual "reduced" or semiclassical notation (cf. Eq. IX.3b) has been introduced. Eqs. 1-3 have been found[33] to reproduce accurately the exact (via summation of phases) calculations of Q for several realistic potential functions. Eq. 1 has been employed[31,34] in the analysis of experimental extrema data assuming a L.-J.(12,6) function[34] and Eqs. 1-3 in connection with a Kihara potential[33].

For the L.-J.(12,6) potential it has been shown[31] that the maximum reduced phase may be approximated by the expression

$$\eta_m^*(K) = \frac{120\pi}{847} \cdot \left(\frac{231}{160}\right)^{1/6} \cdot K^{-1} g(K) = \frac{0.4732}{K} \cdot \left[1 - \frac{1}{4K^{1/2}} + \cdots\right] \tag{X.4}$$

for $K \gg 1$, so that

$$\eta_m \cong 0.4732\, D\, (1 - D/4B^{1/2}) \tag{X.5}$$

where $D \equiv B/A = 2\epsilon\sigma/\hbar v = \dfrac{C^{(6)}}{2\hbar v \sigma^5}$.

Thus the extremum condition in $\Delta Q/\bar{Q}$ may be expressed (in this case):

$$N - \tfrac{3}{8} = 0.3012\, \frac{\epsilon\sigma}{\hbar v_N} \left[1 - \frac{0.354}{v_N}\left(\frac{\epsilon}{\mu}\right)^{1/2} + \cdots\right] \tag{X.6}$$

where v_N is the velocity of the Nth extremum; thus a plot of $N - \frac{3}{8}$ vs v_N^{-1} should pass through the origin (serving to confirm the index assignments) with the initial slope yielding the $\epsilon\sigma$ product (cf. Fig. 14) or, alternatively, the ratio $C^{(6)}/\sigma^5$.

For other potentials Eqs. 4 and 5 differ somewhat (although the dependence of the leading term in Eq. 14 is completely general, following from the v^{-1} functionality of the JB phase shift (Eq. IV,b.3)). Thus a slightly different form of Eq. 15 results in each case. In Ref. 33 tabulations of $\eta_m^*(K)$, β_m and θ_0' are presented for the Kihara (12,6) potential with different values of the parameter α $(-0.3 \leq \alpha \leq 0.5)$, including $\alpha = 0$, the L.-J. (12,6) case; these may be employed in expressions for the deviation function $\Delta Q/\bar{Q}$. In any case, extrema plots of $N - \frac{3}{8}$ vs. v_N^{-1} are all characterized by a limiting linear behavior as $v_N^{-1} \rightarrow 0$.

The oscillatory graphs of $\Delta Q/\bar{Q}$ vs. $1/v$ have been termed [31b] elastic atom-atom impact spectra. In such a plot (cf. Fig. 14) the extrema are approximately evenly spaced (at high velocities) so that the indexing of the extrema is readily accomplished. For a (realistic interatomic) potential with an asymptotic r^{-6} form, if one plots, as a function of v^{-1}, the "apparent" value of the potential constant, $C_{app}^{(6)}$, calculated from Q via Eq. X.9:

$$C_{app}^{(6)} = 5.676 \times 10^{-30}\, v\, Q^{5/2} \tag{16}$$

(where v, Q and C are in cgs units), one obtains a similar oscillatory "spectrum". The average value of $C_{app}^{(6)}$ over the thermal energy range is the true value of $C^{(6)}$. Thus, velocity-averaging in effect eliminates the influence of the short-range forces upon the total elastic scattering cross section, enabling one to evaluate the long-range attractive constant $C^{(6)}$ directly.

After assignment of indices it is possible to ascertain <u>absolute</u>

<u>experimental</u> <u>values</u> of the maximum phase, η_m, as a function of v or k from Eq. XI.1. The experimental results may then be concisely expressed in the form of an expansion of η_m in powers of v^{-1}, say:

$$\eta_m = a_1 v^{-1} - a_2 v^{-2} + \ldots\ldots \tag{17}$$

where

$a_1 = c\, C^{(6)} r_m^{-5}$, with c a numerical constant dependent on the assumed functional form of the potential. Thus, since elastic atom-atom impact spectra yield both $C^{(6)}$ and a_1 (and with less accuracy, a_2), for a given functional form of V(r) it is possible to evaluate r_m (and thus ϵ).

XII. Maxima in Impact Spectra and the Bound States[31]

The relationships between differential and total elastic cross sections, extrema-velocities (and amplitudes) and the interaction potential have been discussed in previous sections. Given a two-body potential function thus derived from scattering experiments, it is only a matter of straightforward computation[35] to evaluate the energy levels corresponding to all the discrete, vibration-rotation states of the composite system. There is also a well-known relation[14] between the bound-state energies and the poles in the scattering amplitude as a function of k, the (complex) wavenumber, occurring in the upper half-plane.

However, only recently has it been pointed out[31] that a rather direct relationship exists between the bound states and the extrema in the total cross sections, i.e., that the maxima in the elastic atom-atom impact spectra serve as "counters" of the vibrational states of the di-atom.

A brief outline of this development follows. Assuming the usual semiclassical conditions it is seen that the maximum phase increases monotonically with decreasing k, while the angular momentum quantum number corresponding to the maximum phase (i.e., L_0, or ℓ_m) decreases smoothly to zero as $k \to 0$. Thus, as the wavenumber is decreased η_m approaches progressively closer to the s-wave ($\ell = 0$) phase shift, $\eta_0(k)$. This, in turn, approaches its zero-velocity limit according to Levinson's theorem[36]:

$$\lim_{k \to 0} \eta_0(k) = n_0 \pi \qquad \text{(XII.1)}$$

Here n_0 is the number of discrete levels of zero angular momentum, i.e., the number of (rotationless) vibrational states of the di-atom. As discussed in the previous section, a maximum in the impact spectrum occurs once for each time $\eta_m(k)$ passes through integral multiples of π (more accurately, when $\eta_m = \frac{5}{8}\pi, \frac{13}{8}\pi,$ etc.); thus the total number of maxima should equal the number of bound states, n_0.

Unfortunately, the semiclassical approximations become less valid as k is decreased. In addition to the onset of the violently non-classical orbiting-tunneling phenomenon at low energies, another difficulty arises due to the failure of the statistics for the random-phase approximation (we recall that the number of non-negligible phases is roughly $2kr_0$, so that for $kr_0 \lesssim 10$ the rph assumption has no validity). Thus the above bound-state relation is not a rigorous one; indeed we may anticipate a certain degree of sharp "fine structure" in the impact spectrum at sub-thermal energies, probably unresolvable experimentally. Nevertheless, there remains a rigorous and direct correlation[31b] between the low-index (high k) extrema and the low-lying vibrational states (quantum number v):

$$N-1 \longleftrightarrow v \qquad \text{(XII.2)}$$

A re-statement of the bound-state rule which should be suitable for application in any experimentally feasible situation is as follows:

The observation of m maxima in the elastic atom-atom impact spectrum implies the existence of at least m vibrational states for the di-atom.

The preceding considerations have been applied[34] to experimental extrema observations. In all cases for which the "capacity" of the well for bound states (n_o) was known from the potential parameters it was found that $m \leq n_o$ (neither the number of maxima observed nor the highest index assigned exceeded the theoretical capacity, n_o).

It is clear that the above "level-counting" technique is not dependent on the detailed shape of the potential (so long as the well has a "capacity" for one or more bound states) and should be generally applicable to systems[*] involving ground state atoms, metastables and/or ions.

- - - - -

[*] Extension to systems involving molecules involves certain obvious complications, including inelastic effects. Cf. Sec. XIII.

- - -Examples of systems (other than those analyzed in Ref. 34) for which scattering-bound state experiments and/or calculations of this type have been carried out are as follows:

K $(^2S_{1/2})$	+	Kr $(^1S_0)$	$\rightarrow$	KKr $(^2\Sigma^+)$ [37]	(exp. + calcs.)
Li $(^2S_{1/2})$	+	Hg $(^1S_0)$	$\rightarrow$	LiHg $(^2\Sigma^+)$ [38]	(exp. + calcs.)
He $(^3S_1)$	+	Xe $(^1S_0)$	$\rightarrow$	HeXe $(^3\Sigma^+)$ [39]	(exp.)
He $(^1S_0)$	+	Li^+ $(^1S_0)$	$\rightarrow$	$HeLi^+$ $(^1\Sigma^+)$ [40]	(calcs.)

- --- - -

XIII. Influence of Concurrent Inelastic Processes.

The subject of inelastic collisions of atoms and molecules is not within the scope of the present chapter. Nevertheless it seems worthwhile to consider briefly the question of the influence of concurrent inelastic scattering upon the elastic scattering behavior of molecules.

The simplest situation is the one in which the scattering is inelastic but non-reactive. Here it is known that rotational excitation (and de-excitation) is the most probable path of energy transfer between translation and internal modes. Takayanagi[41] has recently reviewed in great detail the theory of rotational (and vibrational) transitions in molecular collisions. For the purpose of illustration here we shall confine our attention to the special case of the atom-diatomic molecule system[*] following the S-matrix formalism of Arthurs and Dalgarno[42] for scattering by a rigid rotor.

- - - - -

* Detailed calculations for the system He-H_2 have been carried out by Roberts[43]. In addition, the formal procedure[42] has been generalized by Davison[44] to the diatomic-diatomic case, who presented calculations for the H_2-H_2 pair.

- - - - -

The total cross section for the transition $j \rightarrow j'$ may be expressed:

$$Q(j';j) = \frac{\pi}{k^2} \sum_{J=0}^{\infty} (2J+1) \cdot P_{j';j}(J) \qquad \text{(XIII-1)}$$

where the transition probability is

$$P_{j';j}(J) = \frac{1}{2j+1} \cdot \sum_{l=|J-j|}^{J+j} \sum_{l'=|J-j'|}^{J+j'} \left| \delta_{\alpha\beta} - S^{J}_{\beta;\alpha} \right|^2 \qquad \text{(XIII-2)}$$

Here J is the total angular momentum quantum number (conserved in the collision) and $S^{J}_{\beta;\alpha}$ the S-matrix element for the transition from state $\alpha \equiv j, l$ to state $\beta \equiv j', l'$ at given J, defined in terms of a radial wave function with asymptotic form:

$$G_J^{\beta;\alpha}(r) \sim \delta_{\alpha\beta}\, e^{-i(kr - l\pi/2)} - \left(\frac{v}{v'}\right)^{1/2} S^{J}_{\beta;\alpha} \cdot e^{i(k'r - l'\pi/2)} \qquad \text{(XIII-3)}$$

(cf. Eq. III.5). Here v is the relative velocity associated with the incident channel $(v = k\hbar/\mu = (2E/\mu)^{1/2}$ as usual) and v' the corresponding outgoing relative velocity, given by

$$v' = v\left[1 - \frac{\Delta E}{E}\right]^{1/2} = k'\hbar/\mu' \qquad \text{(XIII-4)}$$

where ΔE is the endothermicity of the transition and k' is the exit channel wavenumber. The standard expressions for the coupled radial differential equations will not be reproduced here.

Under semiclassical conditions and with the assumption of strong interchannel coupling, a statistical method (analogous to the rph procedure) may be employed[45] to approximate the transition probabilities; one merely calculates the expectation values for the

(mod-squared of the) S-matrix elements. Taking advantage of the unitarity of the S-matrix, one finds that for N_J coupled channels

$$\langle |S^J_{\beta;\alpha}|^2 \rangle = 1/N_J \tag{XIII-5}$$

so that for $\beta \neq \alpha$

$$\langle P_{j';j}(J) \rangle = [(2j+1)\cdot N_J]^{-1} \tag{XIII-6}$$

For $\beta = \alpha$ (elastic scattering) it is found that

$$\langle P_{j;j}(J) \rangle = (2j+1)^{-1}\cdot \langle |1 - S^J_{\beta;\alpha}|^2 \rangle = (2j+1)^{-1}\cdot(1 + N_J^{-1}) . \tag{XIII-7}$$

From these results it follows that the total (elastic plus inelastic) cross section for scattering to all energetically open channels from state j , i.e., $Q_j^{tot} \equiv \sum_{j'} Q(j';j)$, is independent of the number of coupled channels and is given (approximately) by a formula identical to the Massey-Mohr rph formula (Sec. X) (which referred, of course, to the total <u>elastic</u> cross section in the absence of inelastic scattering). Alternatively expressed, it is found that the elastic cross section is reduced* by an amount just equal to the inelastic cross section, such that

$$Q_j^{tot} = Q_j^{el} + Q_j^{inel} \cong Q_{MM} \tag{XIII-8}$$

- - - - -

*Since the ratio

$$\left[\sum_{j'} \langle P_{j';j}(J) \rangle\right] / \langle P_{j;j}(J) \rangle \leq 1, \tag{XIII-9}$$

from Eqs. 5 and 6, the total inelastic cross section can never exceed the total elastic cross section, i.e.

$$\frac{Q_j^{inel}}{Q_j^{el}} \leq 1 \quad \text{and} \quad \frac{Q_j^{inel}}{Q_j^{tot}} \leq \frac{1}{2} \quad . \qquad \text{(XIII-10)}$$

This result, i.e., "conservation" of total cross section, obtained with a minimum of restrictive assumptions, may well have general validity (e.g., extension to the polyatomic case, as well as inclusion of vibrational excitation) in the field of non-reactive molecular scattering.

For the most general case in which chemically reactive scattering is concurrent, the situation is, of course, much more complicated. Reactive scattering is always accompanied by elastic scattering (as well as inelastic transitions) so a rigorous treatment is expected to be formidable. It is not appropriate here to review the literature in what may be termed the fundamentals of chemical reaction kinetics, but it is relevant to reference the basic collision-theory treatment of Eliason and Hirschfelder[46] (which introduced the concept of the "multichannel" differential chemical reaction cross section) and the important S-matrix formulation of Smith[47]. It appears, however, that the question of the influence of the reactive scattering upon the elastic scattering has not yet been considered in detail[50]

In order to obtain a qualitative answer to this question we explore the utility of the optical model for reactive scattering. Here the interaction potential is assumed complex:

$$V(r) = V_0(r) + i\,W_0(r) \qquad \text{(XIII-11)}$$

with the imaginary part responsible for the absorption (i.e., reaction). Without speculating here on the origin or functional form of $\mathrm{Im}\,V(r)$ we merely recognize[6,14] that the inclusion of this term will yield complex phase shifts and thus reactive scattering.

We make use of the phenomenological "diffraction theory" treatment of Greider and Glassgold[48]. To begin with, we consider as a first approximation the "black-sphere" model (developed long ago for the scattering of neutrons by nucleons)[*].

- - - - -

[*] See, for example, Ref. 14, Sec. 117; the small-angle result is the same as that of Ref. 48, Eqs. V-1,2 for simple diffraction scattering.

- - - - -

Starting with

$$f(\theta) = \frac{1}{2ik}\sum_{\ell}(2\ell+1)\cdot(S_\ell - 1)\cdot P_\ell(\cos\theta) \qquad \text{(XIII-12)}$$

where $S_\ell \equiv e^{2i\eta_\ell}$, with η_ℓ complex (say $\eta_\ell = a_\ell + i b_\ell$); we have for the total elastic cross section

$$Q^{el} = \frac{\pi}{k^2}\sum_{\ell}(2\ell+1)\cdot|1 - S_\ell|^2 \quad ; \qquad \text{(XIII-13)}$$

for the total reactive (inelastic) cross section

$$Q^r = \frac{\pi}{k^2}\cdot\sum_l (2l+1)\cdot\left[1-|S_l|^2\right] = \frac{\pi}{k^2}\cdot\sum_l (2l+1)\cdot\beta_l \qquad \text{(XIII-14)}$$

(where $\beta_l \equiv 1-|S_l|^2$ is the "opacity") and for the total cross section

$$Q^{tot} = \frac{\pi}{k^2}\cdot\sum_l (2l+1)\cdot\left\{1-|S_l|^2+|1-S_l|^2\right\}$$

$$= \frac{2\pi}{k^2}\cdot\sum_l (2l+1)\cdot\left[1-\mathrm{Re}\,S_l\right] = \frac{4\pi}{k}\,\mathrm{Im}\,f(0)\,. \qquad \text{(XIII-15)}$$

Assuming total absorption for all $l < L \cong kR$ (where R is the sphere radius) and no interaction* for $l \geq L$, we have

$$\begin{aligned} S_l &= 0 \quad \text{for} \quad l < L \\ S_l &= 1 \quad \text{for} \quad l \geq L \end{aligned} \qquad \text{(XIII-16)}$$

so that $$Q^r = Q^{el} = \tfrac{1}{2}Q^{tot} = \frac{\pi L^2}{k^2} \cong \pi R^2\,. \qquad \text{(XIII-17)}$$

- - - - -

* For small angles this leads to a pure imaginary scattering amplitude (n.b.: contrast with the Born approximation result, namely, pure real forward amplitude),

$$f(\theta) \cong \frac{i}{k\theta}\,L\cdot J_1(L\theta) \cong \frac{iR}{\theta}\cdot J_1(kR\theta)\,; \qquad \text{(XIII-18a)}$$

we note that Imf(0) = $L^2/2k$. (XIII-18b)

Thus we have the standard formula for "diffraction scattering":

$$I(\theta)_{diff.} \cong R^2 \cdot [J_1(kR\theta)]^2 / \theta^2 \quad . \qquad \text{(XIII-18c)}$$

- - - - -

Thus it is seen that the black sphere model (Eq. 17) gives the same "conservation" result as Eq. 8, namely

$$Q^{tot} = \frac{2\pi L^2}{k^2} = Q_{rph} = Q^{el} + Q^{inel} \qquad \text{(XIII-19)}$$

(recalling Eq. X.1 for $Q_<$). However, although it is true that the existence of inelastic scattering necessarily implies concurrent elastic (or "shadow") scattering, the earlier restriction $Q^{inel}/Q^{el} \leq 1$ <u>no longer applies</u> in the case of an absorptive (complex) potential with its associated complex phase shifts.

Re-writing (i.e., redefining)

$$S_l = e^{2a_l} \cdot e^{2ib_l} \equiv (1-\beta_l)^{1/2} \cdot e^{i\alpha_l} \qquad \text{(XIII-20)}$$

where α_l and β_l are real (noting that $0 \leq \beta_l \leq 1$) Eqs. 13-15 become

$$Q^{el} = \frac{\pi}{k^2} \cdot \sum_{l=0}^{L} (2l+1) \cdot [2 - \beta_l - 2 \cdot (1-\beta_l)^{1/2} \cos \alpha_l] \qquad \text{(XIII-21)}$$

$$Q^{r} = \frac{\pi}{k^2} \cdot \sum_{l=0}^{L} (2l+1) \cdot \beta_l \qquad \text{(XIII-22)}$$

$$Q^{tot} = \frac{2\pi}{k^2} \cdot \sum_{l=0}^{L} (2l+1) \cdot [1 - (1-\beta_l)^{1/2} \cos \alpha_l] \qquad \text{(XIII-23)}$$

Assuming maximum opacity ($\beta_\ell = 1$), Eqs. 21-23 correctly yield the black sphere results (Eqs. 17 and 19). Also, as expected, assuming zero opacity throughout, $Q^r = 0$ and $Q^{el} = Q^{tot}$. Moreover, if $\langle \cos \alpha_\ell \rangle = 0$, then $Q^{tot} = Q_{rph}$ as it should.

However, an interesting possibility arises for intermediate opacities: namely, it is readily possible to obtain $Q^r > Q^{el}$! For example, assuming $\alpha_\ell = 0$ and β_ℓ constant throughout (independent of ℓ in the range $0 \leq \ell < L$), we have for the ratio of elastic to reactive cross sections:

$$\frac{Q^{el}}{Q^r} = \left[2 - \beta_\ell - 2(1-\beta_\ell)^{1/2}\right] / \beta_\ell \qquad \text{(XIII-24)}$$

so that the inelastic contribution <u>exceeds</u> the elastic for any $\beta_\ell < 1$. The ratio Q^{el}/Q^r decreases toward zero as the opacity is decreased (with a concomitant reduction of the total cross section toward zero, of course, in the limit of $\beta_\ell \doteq 0$). Thus we conclude that it is entirely possible for the total reaction cross section to <u>exceed</u> one-half of the total scattering cross section!

Returning once again to the question of the influence of the reactive scattering upon the elastic cross section, we may immediately obtain an approximate solution if we assume unit opacity for $\ell < L$, while all remaining phase shifts η_ℓ $(\ell \geq L)$ are unaffected, i.e., pure real, and the same as would obtain in the absence of inelastic scattering.

Employing the generalized optical theorem (Eq. 15)

we have

$$Q^{tot} = \frac{4\pi}{k} \cdot Im\, f(0) = \frac{4\pi}{k}\left\{ \left[Im\, f(0)\right]_{<} + \left[Im\, f(0)\right]_{>} \right\} \qquad \text{(XIII-25)}$$

where the first term on the right represents the contribution from $\ell < L$, i.e., the diffraction scattering, and the second one from $\ell \geq L$, i.e., the residual elastic scattering. Provided L is less than the MM-rph "cut-off" angular momentum, we have

$$\left[Im\, f(0)\right]_{>} = \left[Im\, f(0)\right]_{tot} - \frac{L^2}{2k} = \frac{k}{4\pi} Q_{SLL} - \frac{L^2}{2k} \qquad \text{(XIII-26)}$$

while

$$\left[Im\, f(0)\right]_{<} = \left[Im\, f(0)\right]_{black} = \frac{L^2}{2k} \qquad \text{(XIII-26b)}$$

so that

$$Q^{tot} = Q_{SLL} \,. \qquad \text{(XIII-27)}$$

Thus the total cross section is unaffected by the reactive scattering, i.e., we see once again the "conservation" of total cross section. However, in view of the result of Eq. 24 this result cannot be taken as generally applicable. The only conclusion which seems independent of model is expressible by the rather weak inequality

$$Q^{el} = Q^{tot} - Q^{r} \leq Q_{SLL} \,. \qquad \text{(XIII-28)}$$

One related point should be noted, i.e., the significant

influence of the reactive scattering on the wide-angle differential elastic scattering cross section. This is manifested as a loss in the elastically scattered intensity at large angles (corresponding to small impact parameters), predictable on the basis of simple semi-classical considerations*. In terms of the present model, this corresponds to a (rather abrupt) gain in opacity (say, from 0 to 0.9) for angular momentum (impact parameter) less than some critical value.

- - - - -

* This effect has been observed and exploited by Greene and Ross[49], in connection with their reactive scattering studies.

- - - - -

XIV. References

[1] See, for example, a) J. O. Hirschfelder, C. F. Curtiss and R. B. Bird, "Molecular Theory of Gases and Liquids", J. Wiley and Sons, N.Y. 1954; b) E. H. Kennard, "Kinetic Theory of Gases", McGraw-Hill Co. N.Y. 1938.

[2] K. W. Ford and J. A. Wheeler, Ann. Phys. 7, 259, 287 (1959).

[3] E. A. Mason, J. Chem. Phys. 26, 667 (1957).

[4] For references see the chapter by I. Amdur and J. E. Jordan. Also I. Amdur and R. R. Bertrand, J. Chem. Phys. 36, 1078 (1962); I. Amdur, Planetary and Space Sci. 3, 228 (1961); and other papers in the series which began with I. Amdur and H. Pearlman, J. Chem. Phys. 8, 7 (1940).

[5] a) E. A. Mason and J. T. Vanderslice, in "Atomic and Molecular Processes", ed. by D. R. Bates, Academic Press N.Y. (1962); b) T. Y. Wu and T. Ohmura, "Quantum Theory of Scattering", Prentice Hall, N. J. (1962) p. 125; c) H. Pauly, Fort. der Physik 9, 613 (1961).

[6] See, for example a) N. F. Mott and H. S. W. Massey, "Theory of Atomic Collisions", Clarendon Press, Oxford, 2nd Ed. (1949); A. Messiah "Quantum Mechanics", John Wiley and Sons, New York (1962); H. S. W. Massey, Handbuch der Physik 36, 232 (1956); E. H. S. Burhop in "Quantum Theory. I. Elements", Chap. 9, Ed. by D. R. Bates, Academic Press, N.Y. (1961); b) T. Y. Wu and T. Ohmura, Ref. 5b; c) R. B. Bernstein, J. Chem. Phys. 33, 795 (1960); 34, 361 (1961).

[7] See, for example, H. S. W. Massey and R. A. Buckingham, Proc. Roy. Soc. (London) A168, 378 (1938); R. A. Buckingham, J. Hamilton and H. S. W. Massey, ibid. A179, 103 (1951); R. A. Buckingham, A. R. Davies and D. C. Gilles, Proc. Phys. Soc. (London) 71, 457 (1958); R. A. Buckingham and J. W. Fox, Proc. Roy. Soc. (London), A267, 102 (1962).

[8] See, for example, J. DeBoer and A. Michels, Physica 6, 409 (1939); J. DeBoer, Repts. Progr. Phys. 12, 351 (1949); J. DeBoer and E. G. D. Cohen, Physica 17, 993(1951).

[9] See, for example, (a) R. P. Marchi and C. R. Mueller, J. Chem. Phys. 38, 740 (1963); (b) C. R. Mueller and R. P. Marchi, ibid. 38, 745 (1963); (c) W. A. Sanders and C. R. Mueller, ibid. 39, 2572 (1963); (d) C. R. Mueller and J. W. Brackett, ibid. 40, 654 (1964).

[10] See, for example, (a) R. B. Bernstein and K. H. Kramer, J. Chem. Phys. 38, 2507 (1963); (b) R. B. Bernstein, ibid. 38, 2599 (1963).

[11] R. B. Bernstein and F. A. Morse, J. Chem. Phys. 40, 917 (1964).

[12] R. B. Bernstein, J. Chem. Phys. 36, 1403 (1962).

[13] See, for example, B. S. Jeffreys in "Quantum Theory I. Elements", ed. by D. R. Bates, Academic Press, New York (1961).

[14] L. D. Landau and E. M. Lifshitz "Quantum Mechanics", Pergamon Press, London (1959).

[15] D. H. Secrest and J. O. Hirschfelder, Proc. Nat. Acad. Sci. 47, 227 (1961); R. B. Bernstein, unpublished notes, Feb., 1961.

[16] (a) H. S. W. Massey and C. B. O. Mohr, Proc. Roy. Soc. A144, 188 (1934);

(b) ibid. A141, 434 (1933).

[17] H. S. W. Massey and R. A. Smith, Proc. Roy. Soc. A142, 142 (1933).

[18] (a) R. B. Bernstein, J. Chem. Phys. 36, 1403 (1962).

(b) ibid. 38, 515 (1963).

[19] See, for example,

(a) H. and B. S. Jeffreys, "Mathematical Physics", Cambridge Univ. Press., Cambridge, 3rd Ed. (1956).

(b) C. Eckart, Rev. Mod. Phys. 20, 399 (1948).

(c) A. Erdelyi, "Asymptotic Expansions", Dover Publications, Inc. N.Y. (1956).

[20] (a) W. Gröbner and N. Hofreiter, Integraltafeln II. Springer-Verlag, Vienna (1961); by transformation of Eq. 313.14a.

(b) ibid., Eq. 314.15a.

[21] (a) P. J. Groblicki and R. B. Bernstein (to be published); also (b) H. U. Hostettler and R. B. Bernstein, Phys. Rev. Letts. 5, 318 (1960).

[22] (a) F. A. Morse, R. B. Bernstein and H. U. Hostettler, J. Chem. Phys. 36, 1947 (1962); F. A. Morse and R. B. Bernstein, ibid. 37, 2019 (1962).

(b) D. Beck, J. Chem. Phys. 37, 2884 (1962); D. Beck, E. F. Greene and J. Ross, ibid., 37, 2895 (1962); M. Ackerman, E. F. Greene, A. L. Moursond and J. Ross, Ninth Intl. Symposium on Combustion, Academic Press, N.Y. (1963).

(c) E. Gersing, E. Hundhausen and H. Pauly, Z. f. Phys. 171, 349 (1963).

[23] Ch. Schlier, Z. f. Phys. 173, 352 (1963).

[24] S. E. Lovell and J. O. Hirschfelder, unpublished calculations.

[25] R. B. Bernstein, Proc. Third Int'l Conf. on Physics of Electronic and Atomic Collisions, London (1963), North-Holland Publ. Co. (in press): also, Science 144, 141 (1964).

[26] (a) H. Pauly, Z. f. Phys. 157, 54 (1959); (b) R. Helbing, Diplomarbeit, Bonn Univ. (1961); (c) R. Helbing and H. Pauly, Z. f. Phys. 176 (1964) (in press); (d) E. A. Mason, J. T. Vanderslice and C. J. G. Raw, J. Chem. Phys. 40, 2153 (1964).

[27] R. G. J. Fraser, H. S. W. Massey and C. B. O. Mohr, Z. f. Phys. 97, 740 (1935).

[28] L. D. Landau and E. M. Lifshitz, Quantum Mechanics (Pergamon Press, Ltd., London, 1959), p. 416.

[29] See, for example, G. Szegö, "Orthogonal Polynomials", Amer. Math. Soc., New York, N.Y. (1959).

[30] L. I. Schiff, Phys. Rev. 103, 443 (1956).

[31] R. B. Bernstein (a) J. Chem. Phys. 37, 1880 (1962); (b) ibid, 38, 2599 (1963).

[32] P. R. Fontana and R. B. Bernstein, to be published (1964).

[33] R. Düren and H. Pauly, Z. f. Phys. 175, 227 (1963); 177, 146 (1964).

[34] E. W. Rothe, P. K. Rol and R. B. Bernstein, Phys. Rev. 130, 2333 (1963).

[35] (a) H. Harrison and R. B. Bernstein, J. Chem. Phys. 38, 2135 (1963);

(b) C. L. Beckel and J. Nakhleh, ibid. 39, 94 (1963).

[36] (a) P. Swan, Proc. Roy. Soc. (London) A228, 10 (1955);

(b) N. Levinson, Kl. Danske Videnskab. Selskab. Mat.-Fys. Medd. 25, No. 9 (1949).

[37] E. W. Rothe, R. H. Neynaber, B. W. Scott, S. M. Trujillo and P. K. Rol, J. Chem. Phys. 39, 493 (1963).

[38] P. J. Groblicki and R. B. Bernstein, to be published (1964).

[39] E. W. Rothe, R. H. Neynaber and S. M. Trujillo, to be published (1964).

[40] G. G. Weber and R. B. Bernstein, to be published (1964).

[41] K. Takayanagi, Prog. Theor. Phys., Suppl. No. 25, 1 (1963).

[42] A. M. Arthurs and A. Dalgarno, Proc. Roy. Soc. (London) A256, 540 (1960).

[43] W. D. Davison, Disc. Far. Soc. 33, 71 (1962).

[44] C. S. Roberts, Phys. Rev. 131, 209 (1963).

[45] R. B. Bernstein, A. Dalgarno, H. S. W. Massey and I. C. Percival, Proc. Roy. Soc. (London) A274, 427 (1963).

[46] M. A. Eliason and J. O. Hirschfelder, J. Chem. Phys. 30, 1426 (1959).

[47] F. T. Smith, J. Chem. Phys. 36, 248 (1962).

[48] K. R. Greider and A. E. Glassgold, Ann. Phys. 10, 100 (1960).

[49] D. Beck, E. F. Greene and J. Ross, J. Chem. Phys. 37, 2895 (1962); also, elsewhere in this volume.

[50] See, however, D. R. Herschbach and G. H. Kwei, Proc. Third Int'l Conf. on Physics of Electronic and Atomic Collisions, London (1963), North-Holland Publ. Co. (in press).

XV. Figures

Legend for Figures

1. a. Top: Dependence of the deflection function upon the reduced impact parameter $\beta \equiv b/\sigma$, for a L.-J.(12,6) potential; here the reduced relative kinetic energy $K \equiv \frac{1}{2}\mu v_r^2/\epsilon = 1.6$; from tabulations in Ref. 1a. b. Bottom: The corresponding dependence of the semiclassical reduced phase η^* upon the reduced impact parameter β for the same case. Note the minimum in the deflection function at $\beta = \beta_r = 1.52$ rad., (corresponding to a "rainbow angle" $\theta_r = 87°$) and the maximum in the reduced phase curve at $\beta = \beta_m = 1.24$, which is also the first zero of the deflection function.

2. A BC plot for a L.-J. (12,6) potential with K = 1.6. Here $B = \beta^2/2\pi$ and $C \equiv \cos\theta$, so that $I^*(\theta)$ is obtained as the sum of the absolute values of the slopes of the contributing branches. For illustration, at $\theta = 60°$, three branches (a,b and c) contribute; for $\theta = \theta_r = 87°$ only one branch contributes to $I^*(\theta)$.

3. A polar plot of $I^*(\theta)$ for scattering by a L.-J.(12,6) potential with K = 1.6. The outer, (solid) curve corresponds to $I^*(\theta)$ directly; the inner one (dashed) has been plotted as $\frac{1}{10} I^*(\theta)$ Intensities for $\theta < 11°$ are not shown. The rainbow effect at 87° is evident.

4. A log-log plot of $I^*(\theta)$ for scattering by a L.-J.(12,6) potential with K = 1.6 (cf. Fig. 3 for the same case). Note the limiting low-angle linearity consistent with a long-range r^{-6} potential.

5. Plot of $\rho^*(\theta)$, from 0-30°, for scattering by a L.-J.(12,6) potential with K = 1.6 (cf. Figs. 3,4 for same case): The dashed curve is the classical result; the solid curve is a quantum mechanical calculation for the same K, with $B \equiv 2\mu\epsilon\sigma^2/\hbar^2 = 2000$ (or $\Lambda^* \equiv \hbar/\sigma(2\mu E)^{1/2} = 0.14$).

6. Typical radical wave function $G_\ell(r) \propto y(x)$ [solid curve] ; for L.-J. (12,6) potential; here K = 3.2, $\ell = 4$, and $A \equiv k\sigma = 20$, $B \equiv 2\mu\epsilon\sigma^2/\hbar^2 = 125$. (See Ref. 6c). Since $x = r/\sigma$, $\eta^* = \Delta\chi$ (see text). The classical turning point (inner inflection point in the radial wave function) is designated on the figure. The dashed curve is the "reference" wave function, $y \propto Ax \cdot j_\ell(Ax)$.

7. Semilog plot of I(θ) for scattering for a L.-J.(12,6) potential; K = 1.6, B = 125 ($\Lambda^* = 0.56$, A = 14.1), comparing quantum with classical calculations. Note region of rainbow scattering!

8. Semilog plot of I(θ) as in Fig. 7 for K = 0.31, B = 2000 ($\Lambda^* = 0.14$, A = 25). For K $\leq$ 0.8, no rainbow scattering effect (classical orbiting only).

9. Interference pattern, $\rho^*(\theta)$, calculated for scattering by a L.-J.(12,6) potential at constant K = 1.8, with various values of A: 20, 40 and 80, corresponding to values of the quantum parameter $\Lambda^* \equiv 2\pi K^{1/2}/A$ of 0.421, 0.210 and 0.105, respectively. Note the decreasing wavelength of the oscillations (with increase in A) but no significant decrease in the amplitude of the oscillations as the classical limit is approached.

10. a. Correlation of interference spacings $\Delta\theta_{min}$ obtained from

calculations of $\rho^*(\theta)$ obtained from calculations of similar to those of Fig. 7, K = 0.8 and 1.8.

b. Detail for K = 1.8 for various values of A: 10,20,30,40,50,60, corresponding, respectively, to Λ^* = 0.842, 0.421, 0.281, 0.210, 0.168, 0.140. The product $A\Delta\theta$ is plotted vs. θ, and compared with the theoretical curve: $A\Delta\theta = 2\pi/(\beta_a+\beta_m)$ (Eq.VI.6).

11. Plot of the "forward scattering ratio" j vs. A $(\equiv k\sigma)$ for the rigid sphere potential and for the L.-J.(12,6) potential with B = 125.

12. Log-log plot of I(θ) at very low angles, calculated /26d/ according to Eq. 24 (quantum), compared with the classical result. The calculations refer to the K-Hg system at a relative velocity of 6.35×10^4 cm sec^{-1}, assuming $C^{(6)} = 8.1 \times 10^{-57}$ erg cm^6 based on the data of Pauly (Z. angew. Phys. 9, 600 (1957)).

13. Log-log plot of Q(v) calculated for a L.-J.(12,6) potential with B = 125. The straight lines represent the SLL(6) and SLL(12) approximations. (For additional details see Ref. 31a).

14. Extrema plot for L.-J.(12,6) potential, with B = 650. The upper curve shows the dependence of $\Delta Q/\bar{Q}$ on $D(\equiv \frac{B}{A})$ while the lower curve shows the indexing of the extrema. (For additional details see Refs. 25, 31, 34).

Figure 1

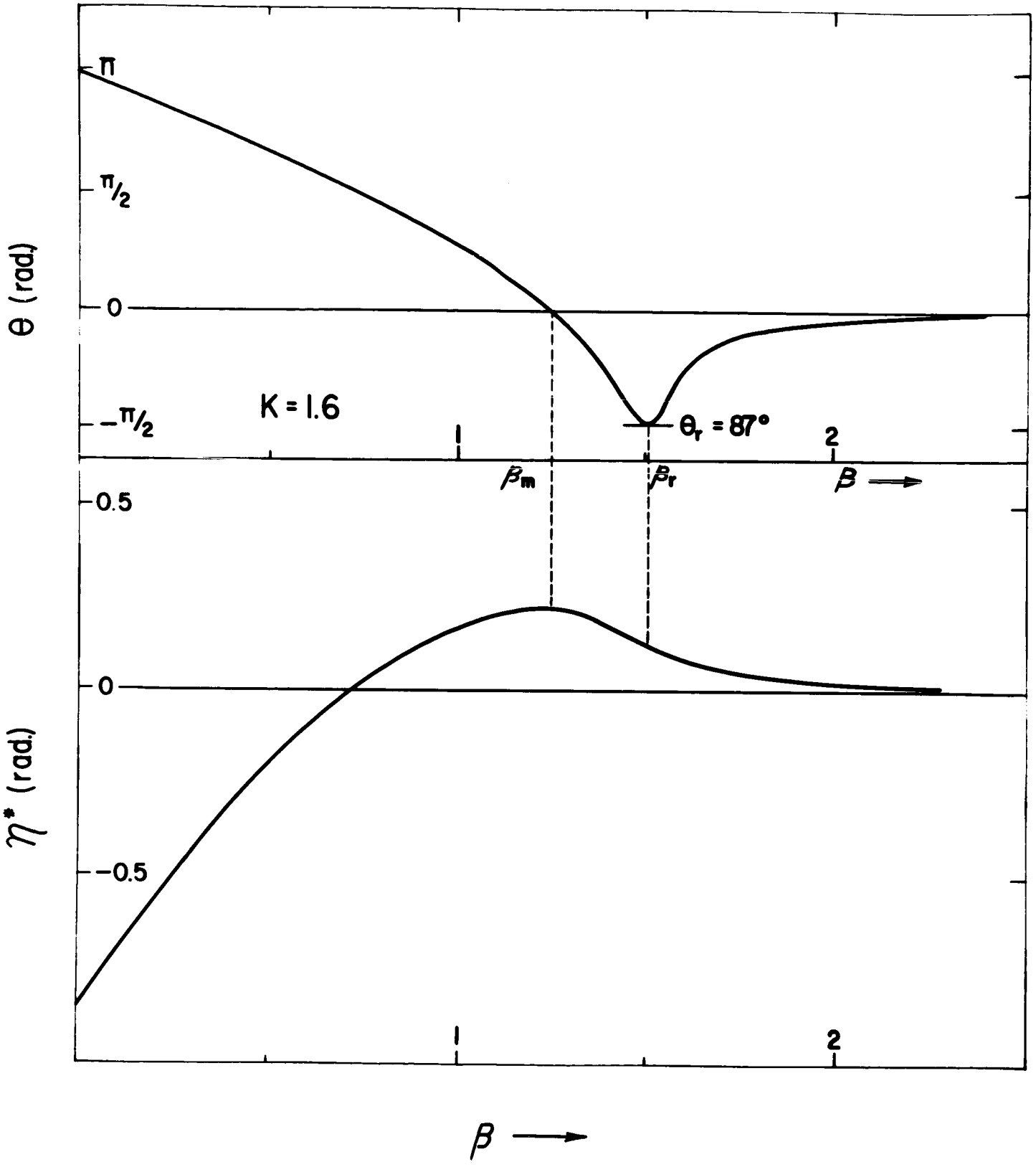

Figure 2

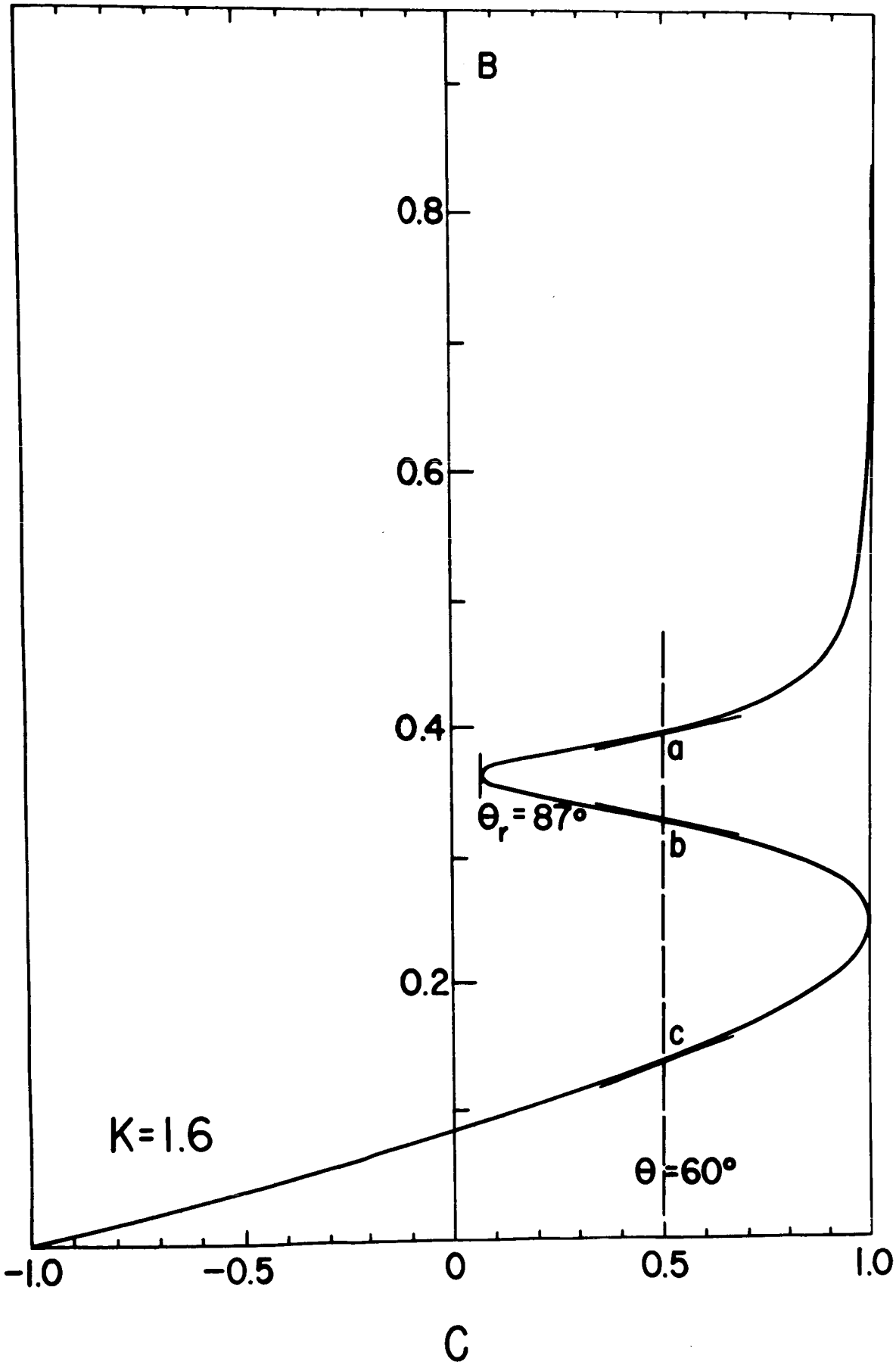

Figure 3

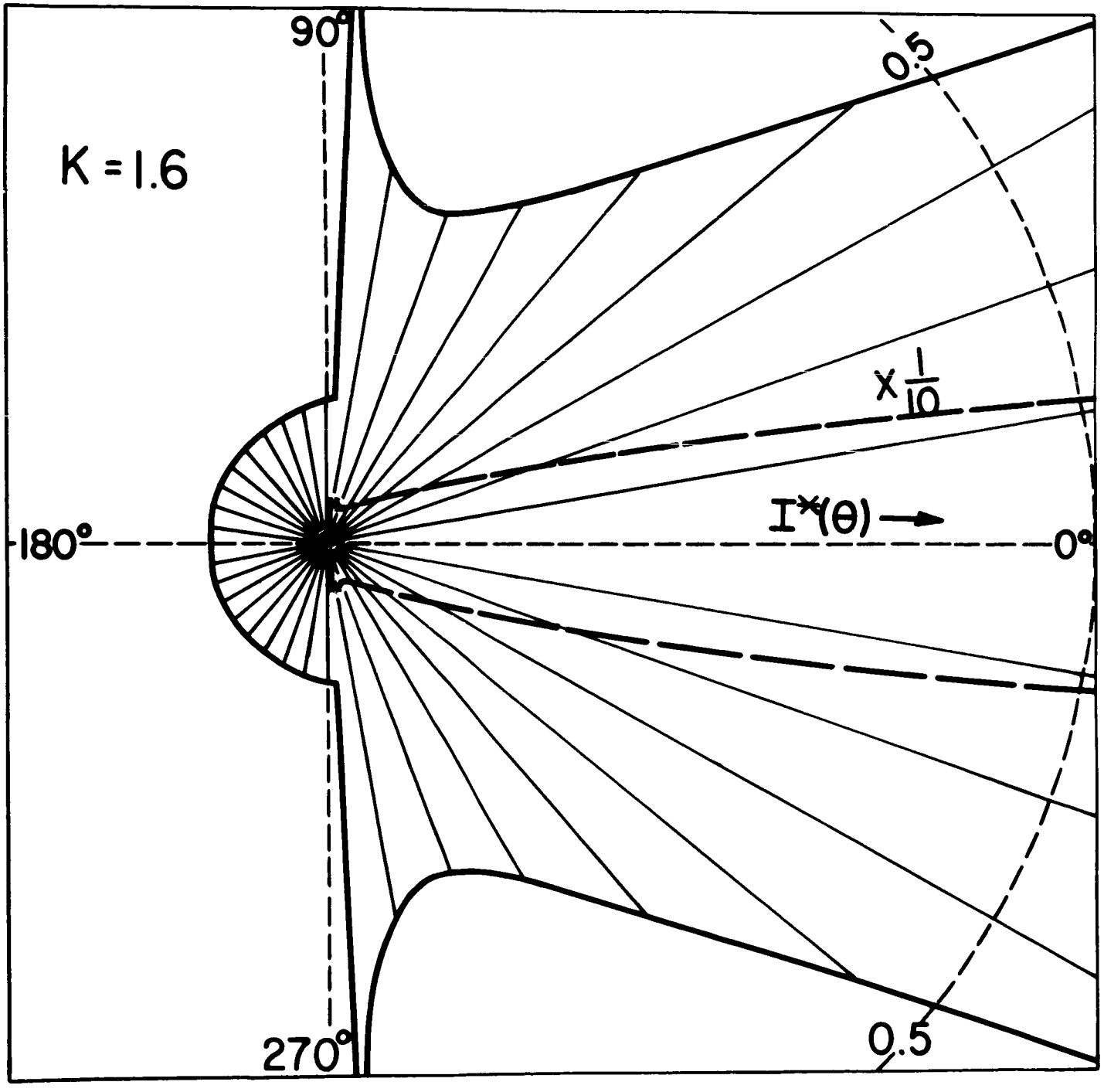

Figure 4

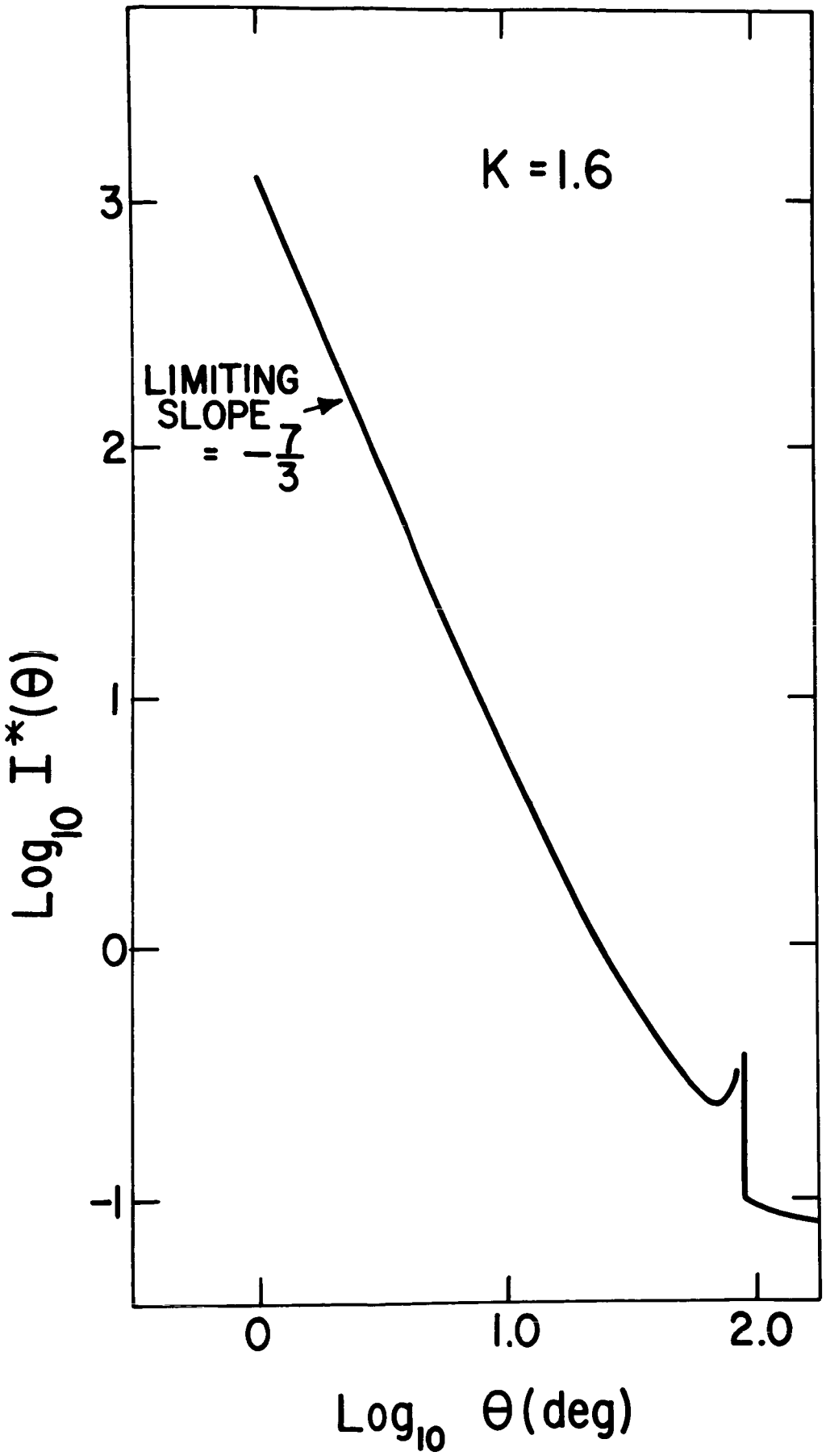
K = 1.6
LIMITING SLOPE = $-\frac{7}{3}$
3
2
1
0
-1
0
1.0
2.0
$\mathrm{Log}_{10}\ I^*(\Theta)$
$\mathrm{Log}_{10}\ \Theta(\mathrm{deg})$

Figure 5

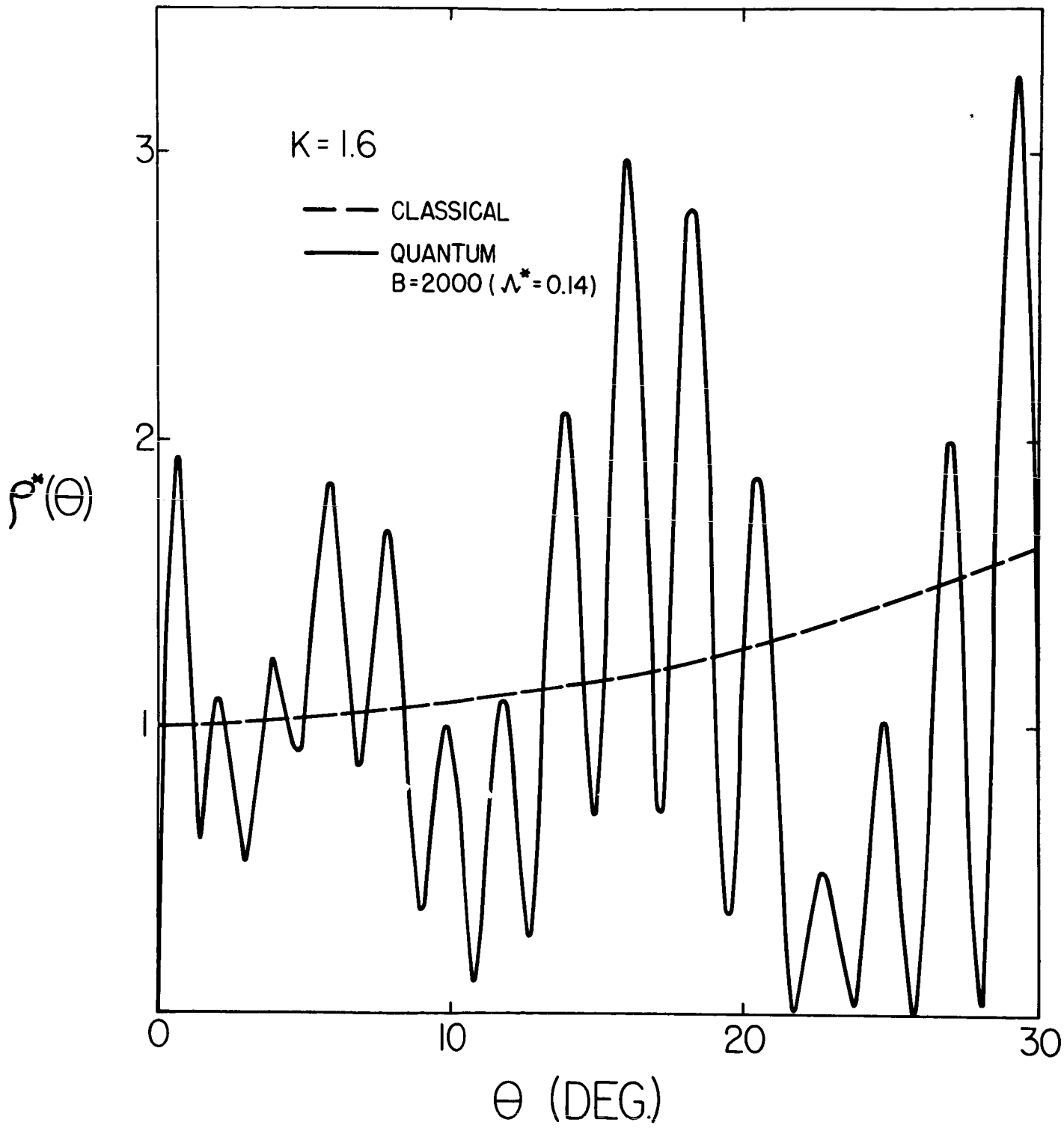

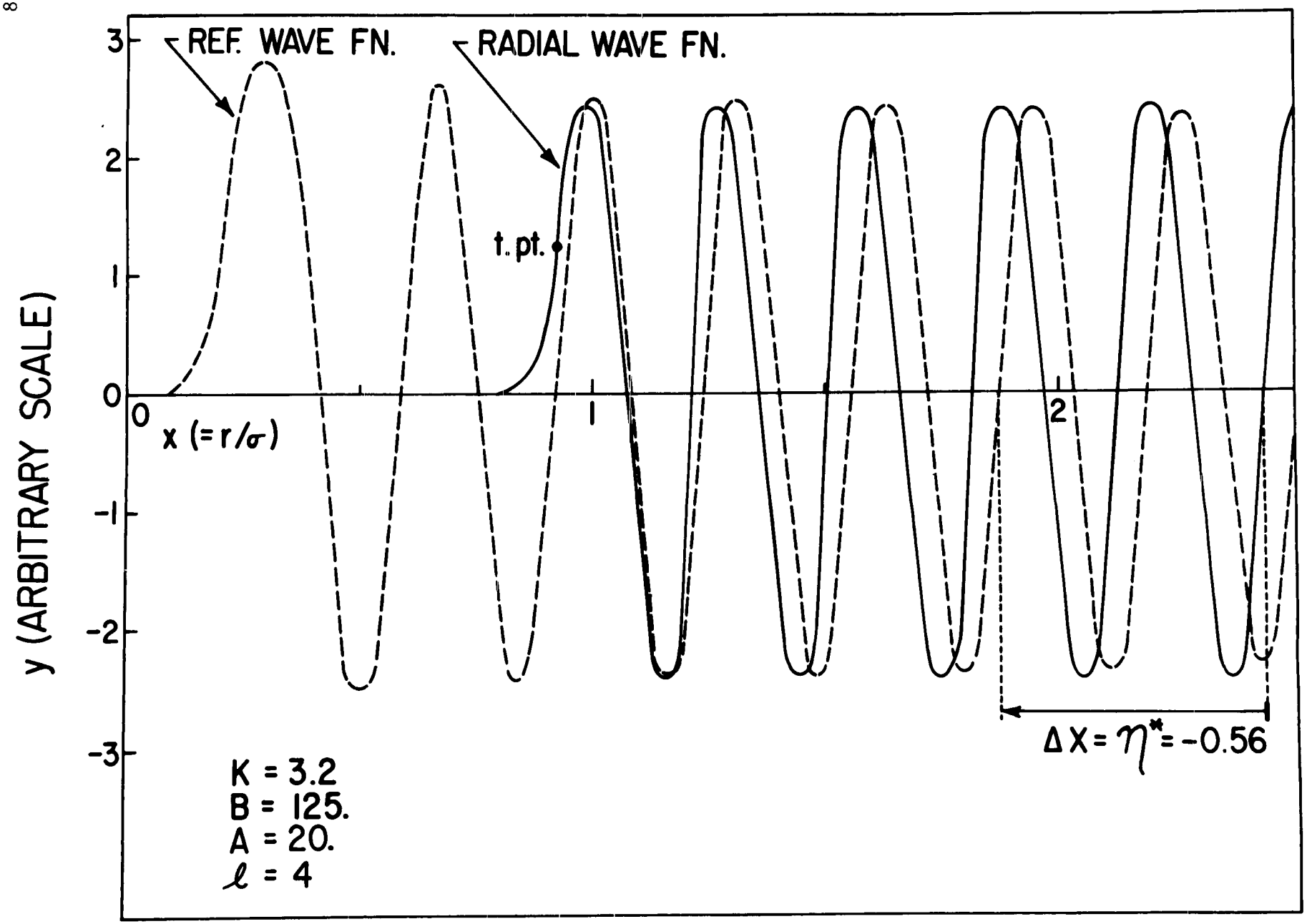
REF. WAVE FN.
RADIAL WAVE FN.
t. pt.
y (ARBITRARY SCALE)
x (= r/σ)
0
1
2
3
-1
-2
-3
ΔX = η* = -0.56
K = 3.2
B = 125.
A = 20.
ℓ = 4

Figure 6

Figure 7

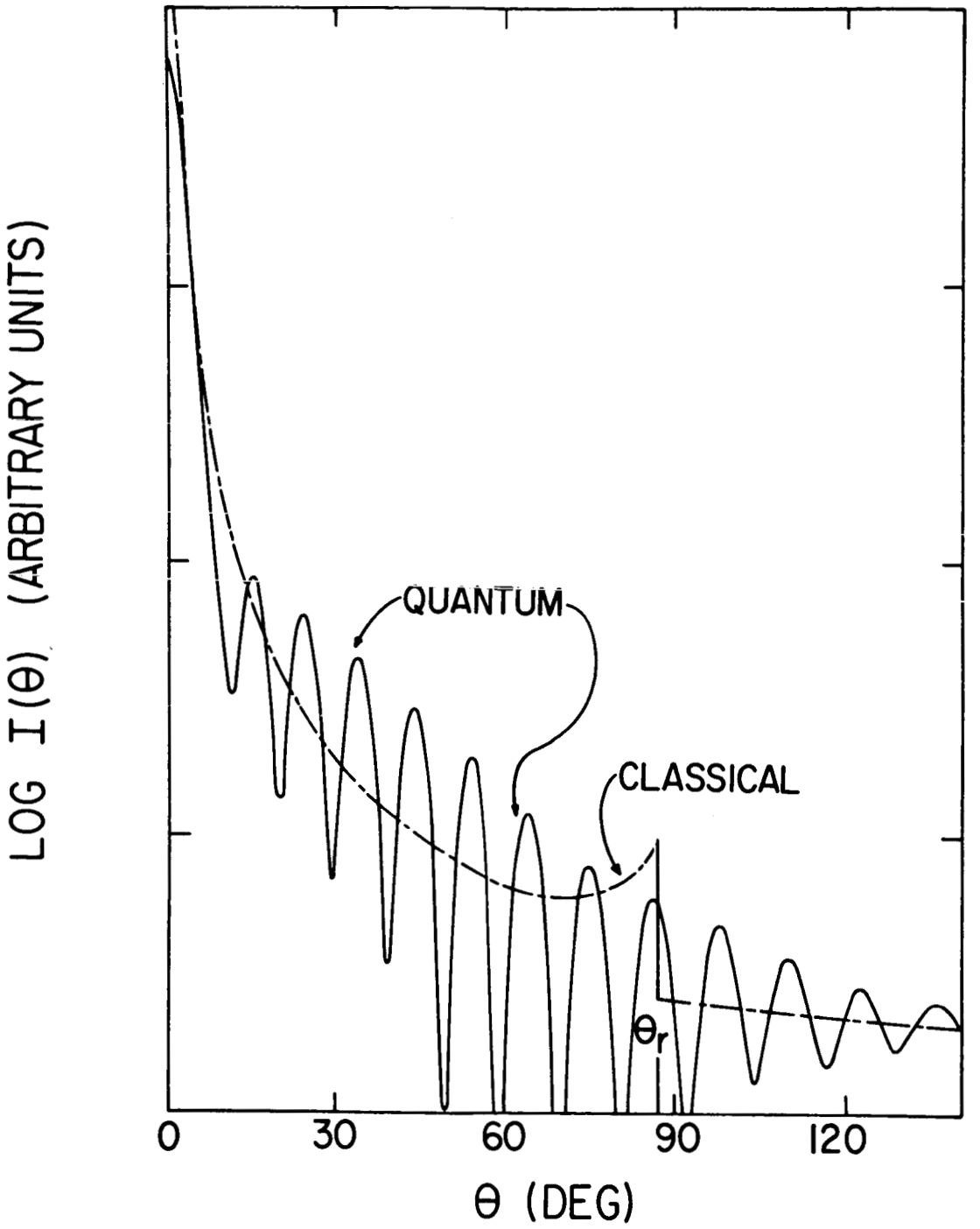
LOG I(θ) (ARBITRARY UNITS)
QUANTUM
CLASSICAL
θr
0
30
60
90
120
θ (DEG)

Figure 8

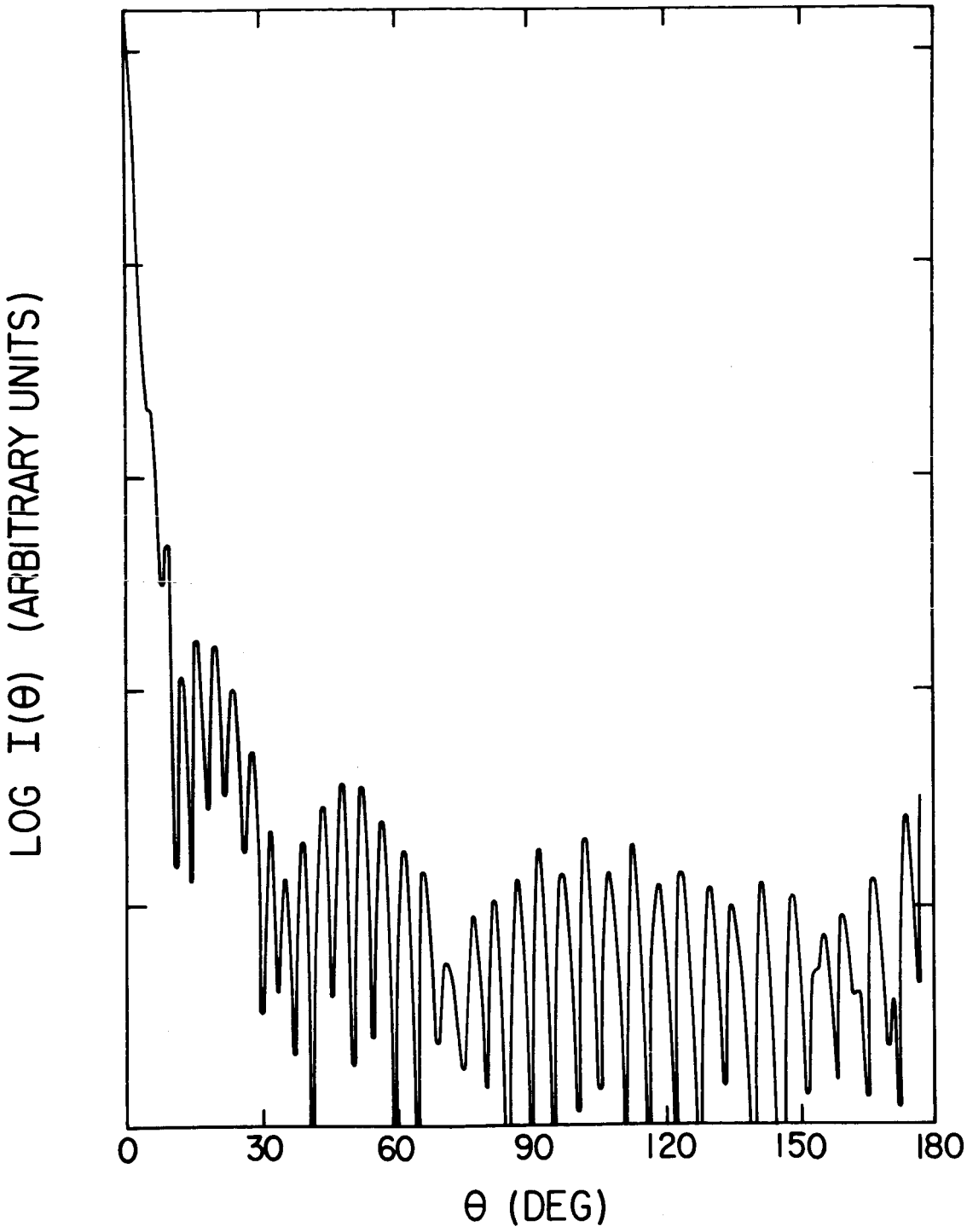

Figure 9

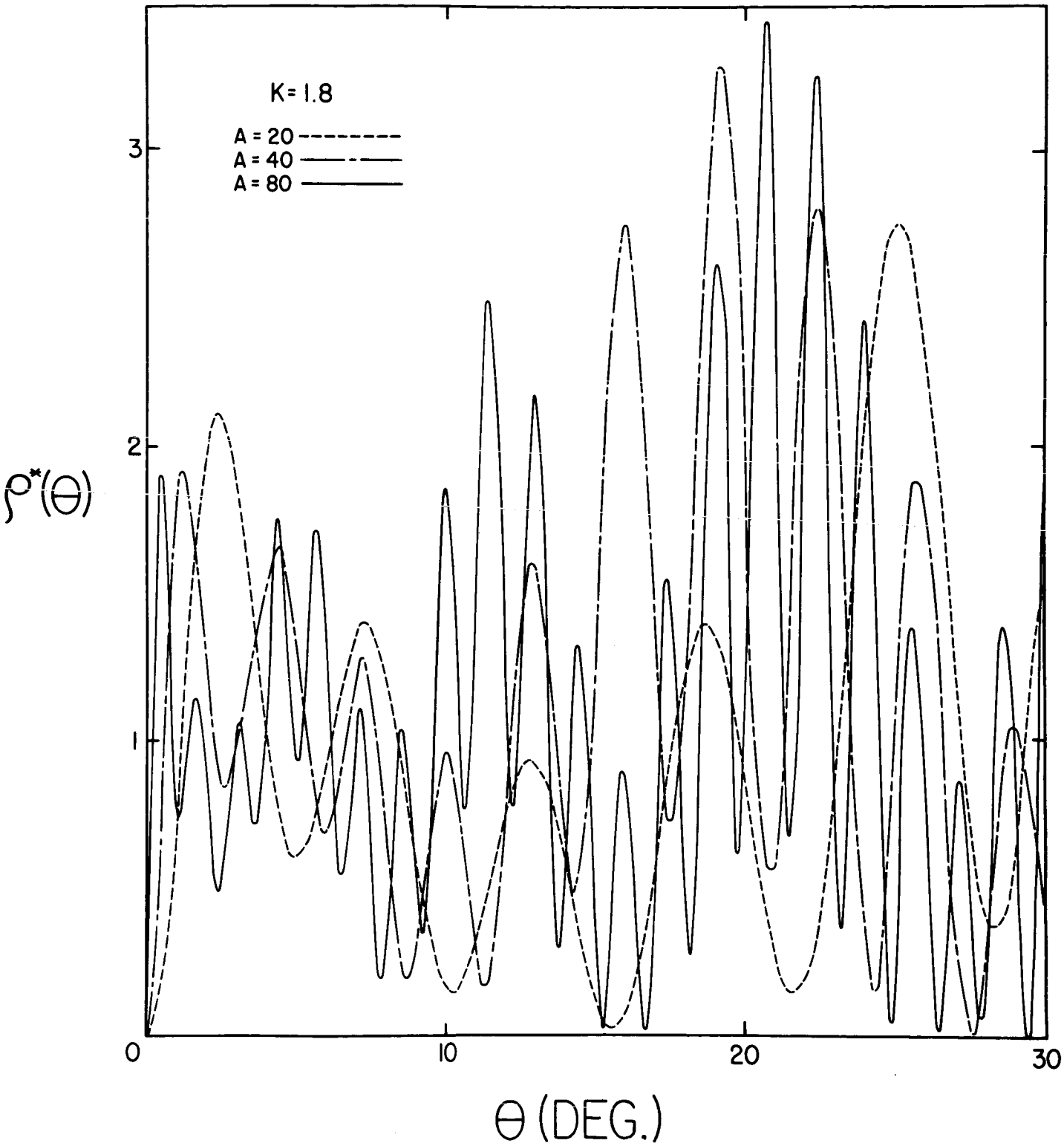

Figure 10a

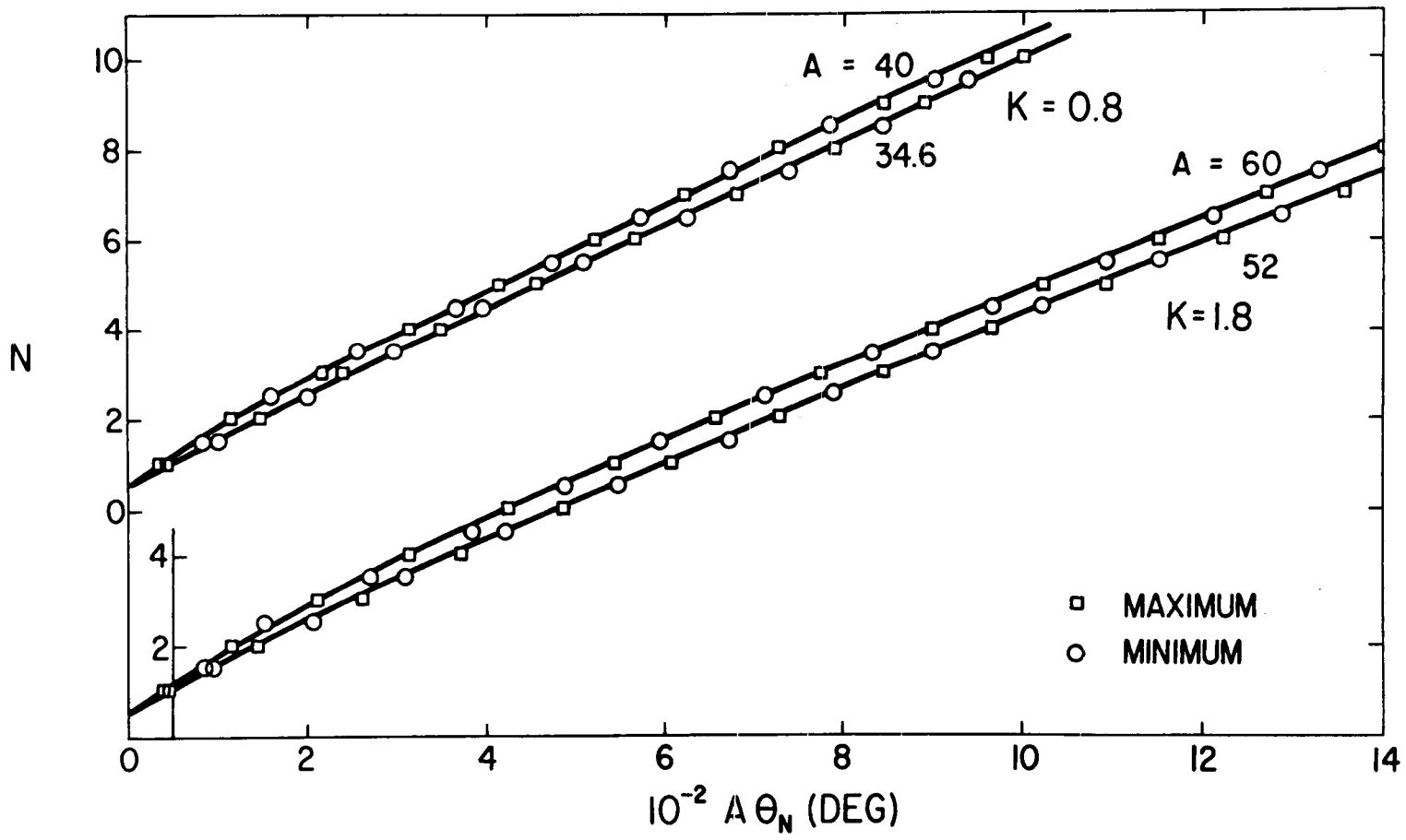
A = 40
K = 0.8
34.6
A = 60
52
K=1.8
MAXIMUM
MINIMUM
N
10^{-2} A Θ_N (DEG)
0
2
4
6
8
10
12
14

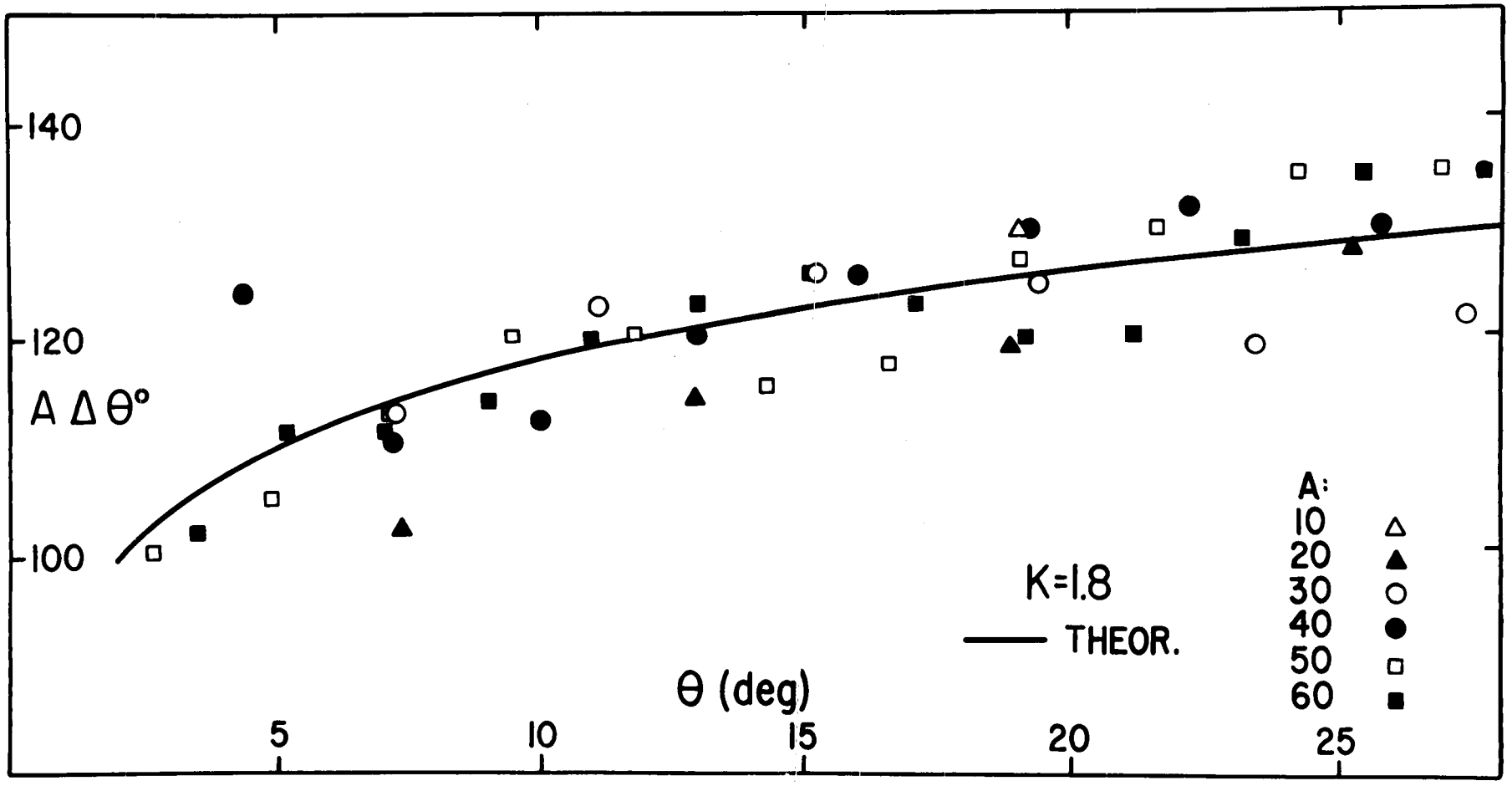

Figure 10b

Figure 11

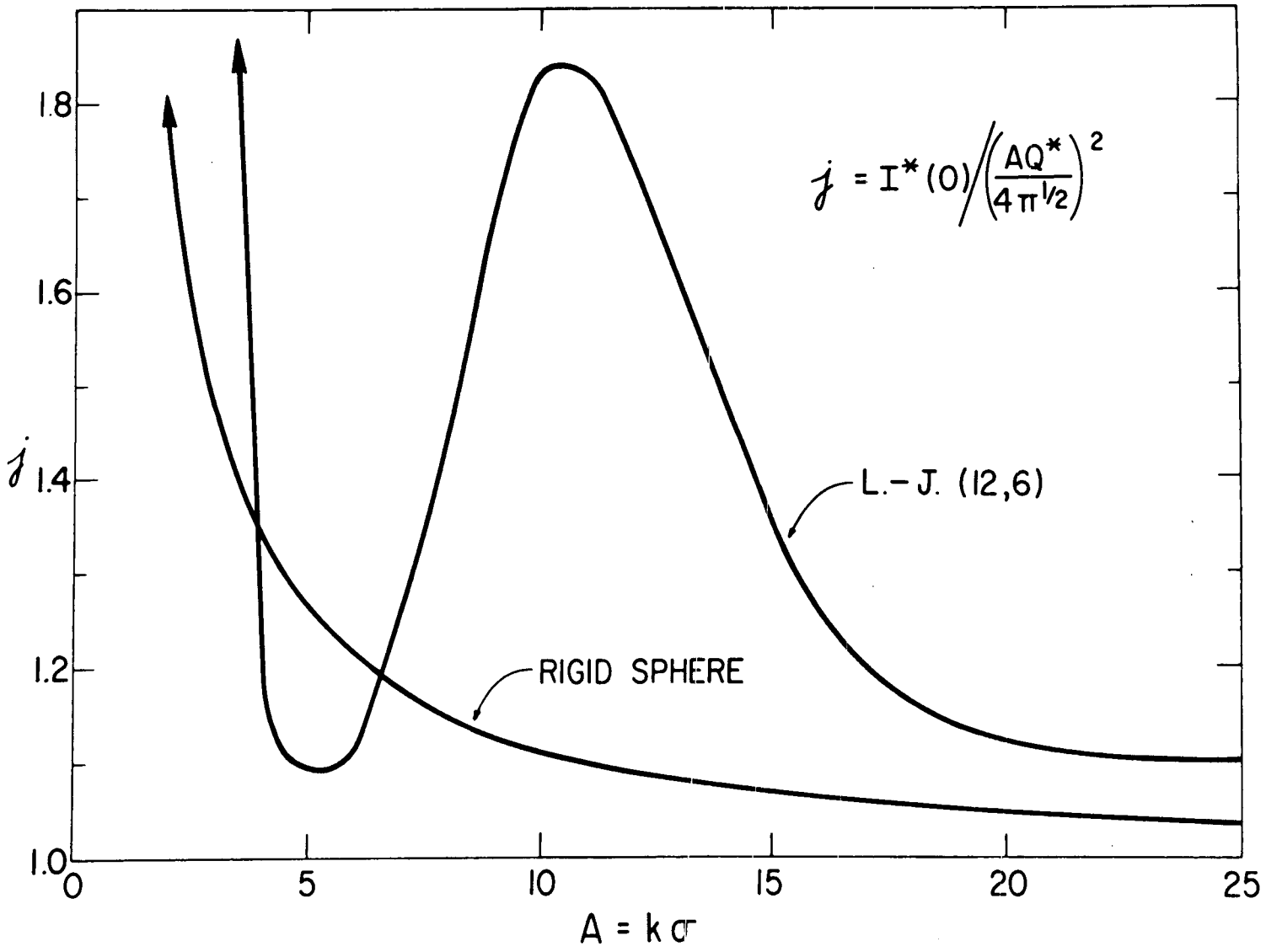
1.8
1.6
1.4
1.2
1.0
j
0
5
10
15
20
25
$A = k\sigma$
$j = I^*(0) \Big/ \left(\frac{AQ^*}{4\pi^{1/2}}\right)^2$
L.-J. (12,6)
RIGID SPHERE

Figure 12

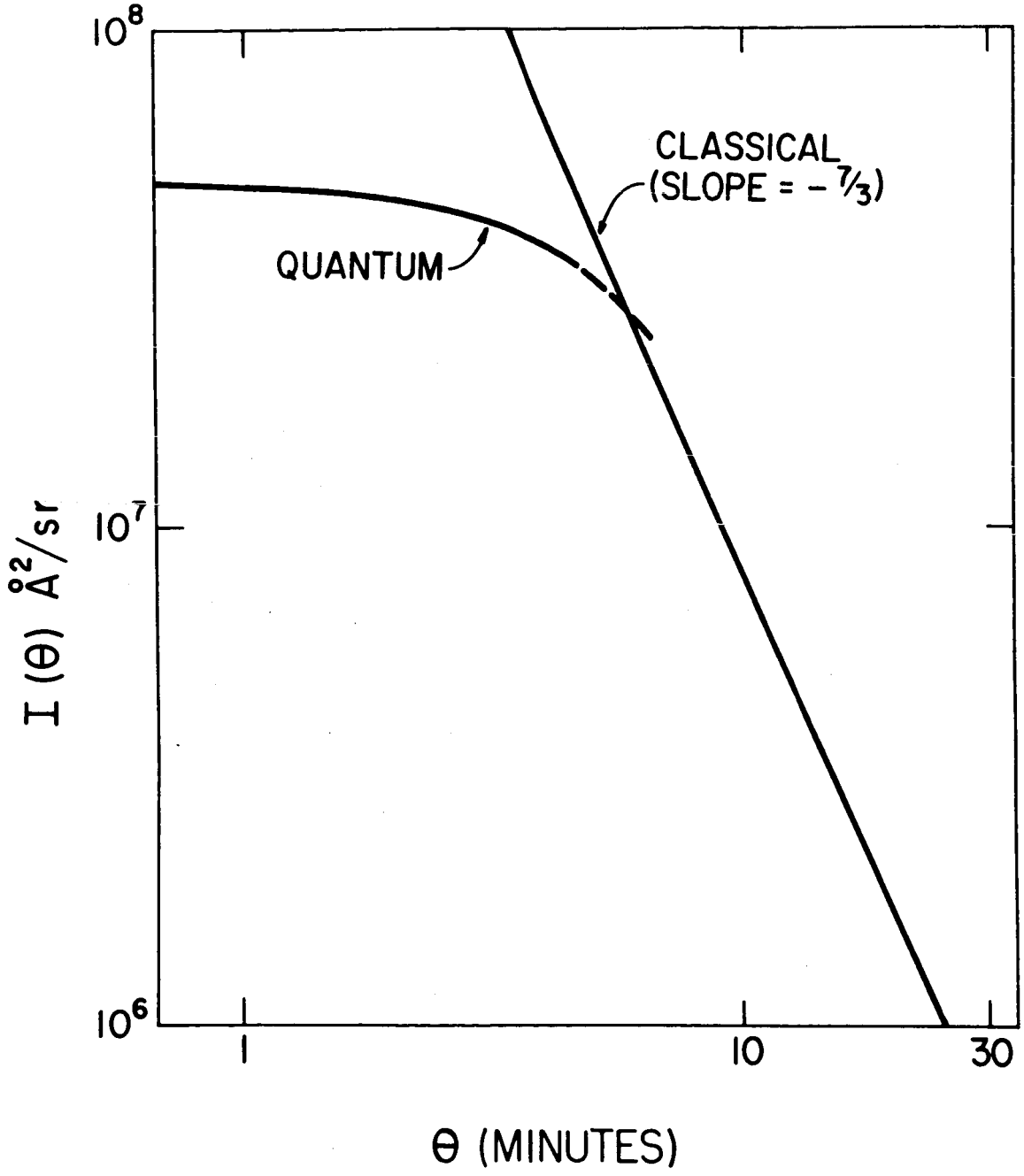
10^8
10^7
10^6
I (Θ) Å²/sr
CLASSICAL
(SLOPE = − 7/3)
QUANTUM
1
10
30
Θ (MINUTES)

Figure 13

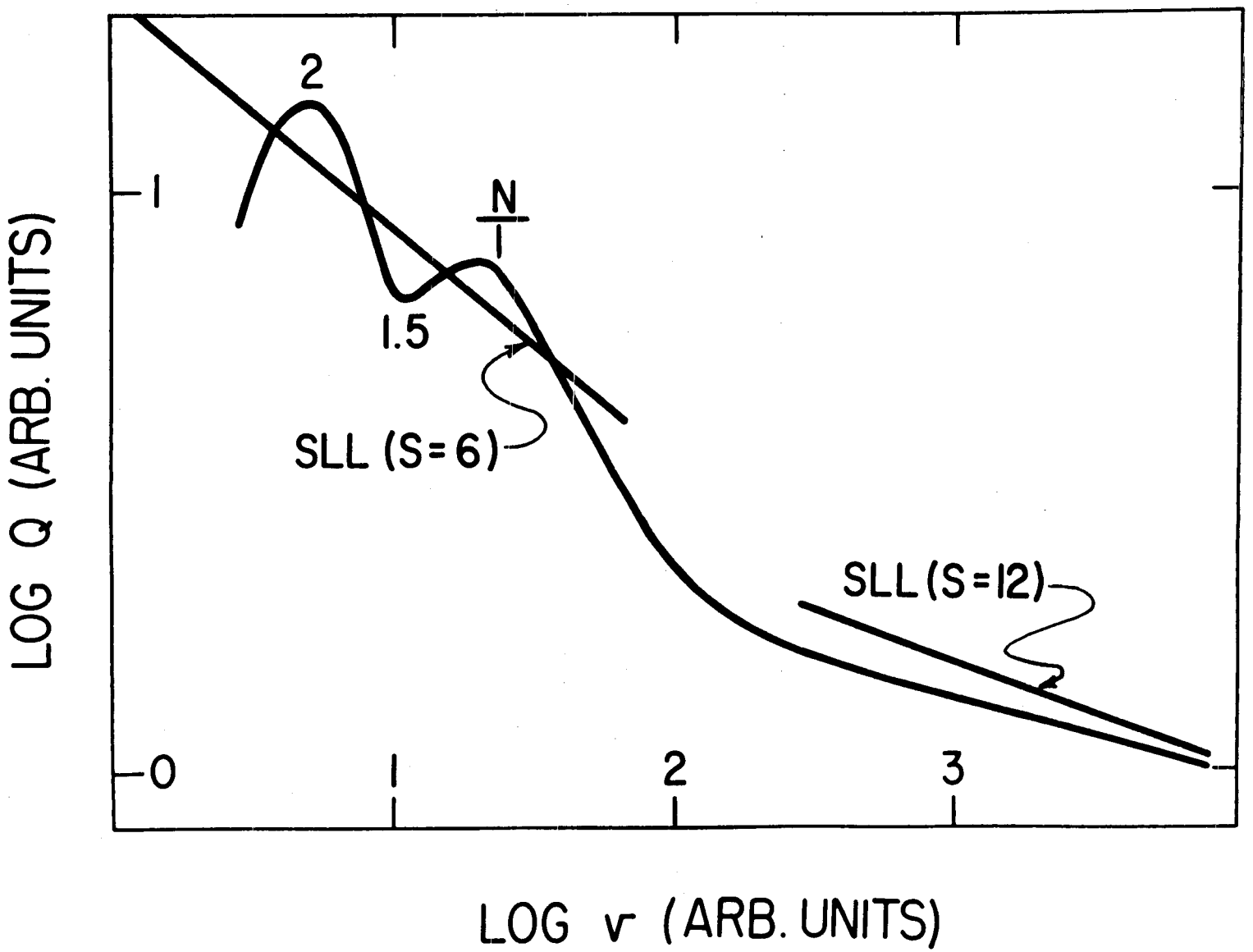
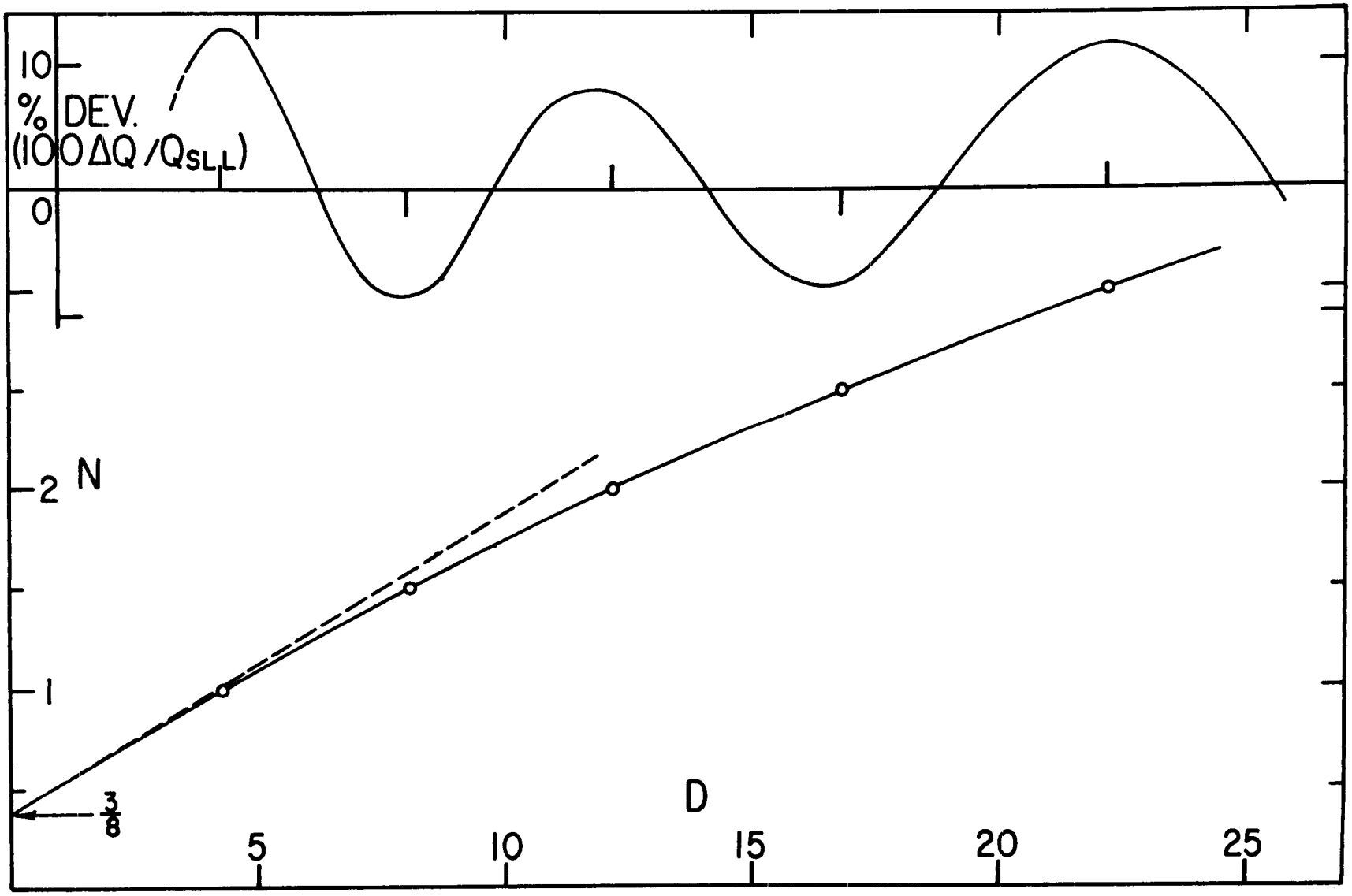
Figure 14